



Deciphering the mechanisms and interactions of the endocrine disruptor bisphenol A and its analogs with the androgen receptor

Rajesh Kumar Pathak^a, Da-Woon Jung^b, Seung-Hee Shin^a, Buom-Yong Ryu^a, Hee-Seok Lee^{b,c,*}, Jun-Mo Kim^{a,**}

^a Department of Animal Science and Technology, Chung-Ang University, Anseong-si, Gyeonggi-do 17546, Republic of Korea

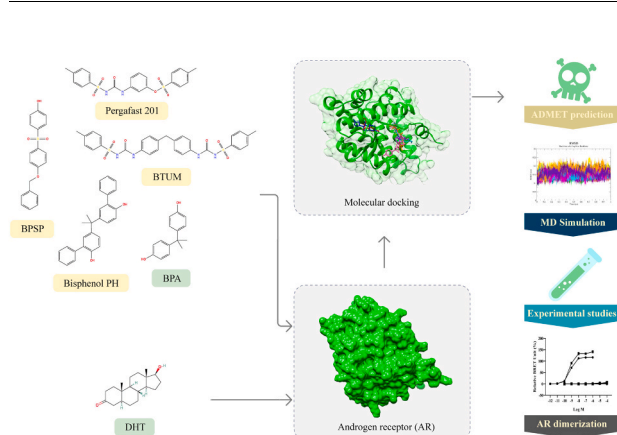
^b Department of Food Science and Technology, Chung-Ang University, Anseong-si, Gyeonggi-do 17546, Republic of Korea

^c Department of Food Safety and Regulatory Science, Chung-Ang University, Anseong-si, Gyeonggi-do 17546, Republic of Korea

HIGHLIGHTS

- BPA and its analogs are hazardous to animal, human, and environmental health.
- The interaction of BPA and its analogs with AR in relation to DHT was studied.
- The molecular interactions were confirmed both computationally and experimentally.
- The binding of BPA and DHT was similar, while its analogs interacted differently.
- Only BPA disrupts DHT-induced AR dimerization, impacting AR function.

GRAPHICAL ABSTRACT



ARTICLE INFO

Keywords:

Androgen receptor
BPA
Endocrine disruptor
Molecular docking
Molecular dynamics simulation

ABSTRACT

Bisphenol A (BPA) and its various forms used as BPA alternatives in industries are recognized toxic compounds and antiandrogenic endocrine disruptors. These chemicals are widespread in the environment and frequently detected in biological samples. Concerns exist about their impact on hormones, disrupting natural biological processes in humans, together with their negative impacts on the environment and biotic life. This study aims to characterize the interaction between BPA analogs and the androgen receptor (AR) and the effect on the receptor's normal activity. To achieve this goal, molecular docking was conducted with BPA and its analogs and dihydrotestosterone (DHT) as a reference ligand. Four BPA analogs exhibited higher affinity (−10.2 to −8.7 kcal/mol) for AR compared to BPA (−8.6 kcal/mol), displaying distinct interaction patterns. Interestingly, DHT (−11.0 kcal/mol) shared a binding pattern with BPA. ADMET analysis of the top 10 compounds, followed by molecular dynamics simulations, revealed toxicity and dynamic behavior. Experimental studies demonstrated that only BPA disrupts DHT-induced AR dimerization, thereby affecting AR's function due to its binding nature. This similarity to DHT was observed during computational analysis. These findings emphasize the importance of

* Corresponding author at: Department of Food Science and Technology, Chung-Ang University, Anseong-si, Gyeonggi-do 17546, Republic of Korea.

** Corresponding author.

E-mail addresses: hslee0515@cau.ac.kr (H.-S. Lee), junmokim@cau.ac.kr (J.-M. Kim).

<https://doi.org/10.1016/j.jhazmat.2024.133935>

Received 29 November 2023; Received in revised form 28 February 2024; Accepted 29 February 2024

Available online 1 March 2024

0304-3894/© 2024 The Authors. Published by Elsevier B.V. This is an open access article under the CC BY license (<http://creativecommons.org/licenses/by/4.0/>).

targeted strategies to mitigate BPA toxicity, offering crucial insights for interventions in human health and environmental well-being.

1. Introduction

Bisphenol A (BPA) is a commercially synthesized chemical compound widely used in the large-scale production of polycarbonate plastics and various everyday plastic-based products. The global annual production of BPA is estimated at approximately 8 billion pounds [19, 76]. BPA is present in numerous everyday items, and some countries have recently banned its use in certain products, such as baby bottles [3], due to concerns regarding its potential adverse effects on human health as an endocrine disruptor [28,44]. Consequently, there has been an increase in the production of BPA analogs that share similar structural or functional properties [28,44,56]. Several BPA analogs have been detected in the environment and various biological and non-biological samples, such as surface water, seawater, blood, urine, milk, vegetables, fruits, honey, dust, sediment, napkins, toilet paper, and textiles [1, 56,77]. Researchers compared the toxic effects of BPA and its analogs, such as bisphenol B (BPB), bisphenol S (BPS), bisphenol F (BPF), and bisphenol AF (BPAF), on zebrafish embryos. They found that the reproductive neuroendocrine toxicity of BPAF closely resembles that of BPA [55]. Certain BPA analogs may also be found in products labeled as “BPA-free”, as their use is not currently regulated or limited [38,60]. However, the safety of these alternatives remains uncertain, as some molecules have demonstrated effects similar to BPA in animal studies, exhibiting endocrine-disrupting activity in both *in vitro* and *in vivo* experiments, sometimes with even higher potency than BPA [4,60].

The estrogenic and antiandrogenic activities of BPA have been widely documented through experimental studies in cell lines and animal models. BPA can bind to the androgen receptor (AR) and disturb its normal activity, directly impacting male fertility [25,58,6,72]. AR comprises three primary functional domains: the N-terminal transcriptional regulation domain, the DNA-binding domain, and the ligand-binding domain [11]. AR undergoes rapid degradation in the absence of ligands. Nevertheless, when androgens bind to the receptor, it gains increased stability. This binding of androgens to the AR's ligand-binding domain induces the separation of the receptor from heat-shock protein 90 (Hsp90) [53,83]. The interaction of AR with BPA and its analogs can affect its normal activity through various mechanisms, including interrupting the natural interaction of androgens, stabilizing AR after binding, dissociating it from Hsp90, and influencing transcription and other biological activities [19].

Studying the interaction of BPA and its analogs with AR is a crucial research area with potential implications for human health [44]. However, several research gaps exist in this field [41,44]. For instance, the interaction of BPA analogs with AR has not been comprehensively studied [59,68]. Additionally, understanding the mechanism of action and effects of continuous exposure to BPA and its analogs, as well as their interaction with AR, is important for public health awareness to minimize potential adverse effects [30,37,65].

Given the harmful effects of BPA analogs, which are promoted as safer alternatives to BPA, there is a need to understand their interactions with AR [39,64]. This understanding can help future research directions and potential solutions [56,70]. In this study, we conducted molecular docking of 22 BPA analogs, including BPA itself, with AR. We also included dihydrotestosterone (DHT), a naturally synthesized androgen hormone, as a reference compound. The goal of this study was to determine their binding energy and identify the specific amino acid residues involved in the interactions. Among the tested compounds, the top 10 that exhibited a strong binding affinity with AR, as well as the reference DHT, were further subjected to ADMET (absorption, distribution, metabolism, excretion, and toxicity) prediction analysis, molecular dynamics simulations (MDS), and Gibbs free energy landscape

(FEL) analysis, followed by experimental studies (Fig. 1). By elucidating the mechanisms through which these compounds interact, we were able to identify the specific amino acid residues in AR that contribute to their binding with BPA and its analogs.

The traditional approach to understanding how hazardous chemicals interact with human molecular targets typically involves experimental methods, such as *in vitro* binding assays, cell culture, and experiments on animal models [21,52,63]. These techniques are aimed at directly observing how hazardous chemicals bind to specific receptors or proteins and their subsequent impact on cellular function and overall health [21]. However, these traditional methods have their limitations; they are often time-consuming, expensive, and require significant resources [14,80]. Moreover, they may not fully capture the complexity of interactions. An alternative to these traditional methods is the use of computational approaches, such as molecular docking, structure-based virtual screening, and MDS [43,48]. These computational methods rely on computer algorithms and models to predict the binding affinity and dynamics of interactions between hazardous chemicals and their target receptors [43]. They can also predict the dynamic behavior of receptor-ligand complexes and provide insight into the amino acid residues of the receptor involved in interactions with hazardous chemicals [48]. Therefore, the current approach offers several advantages over traditional methods for deciphering the interaction between bisphenols and AR. These advantages include speed, cost-effectiveness, and insights into molecular mechanisms. In the present study, the interactions between relevant BPA compounds and AR, predicted through computation, were further validated through experimental studies using a bioluminescence resonance energy transfer (BRET)-based assay.

Investigating the relationship between BPA and its analogs with AR is one of the most important, timely, and significant areas of current scientific research [7,70]. Given how common these substances are in everyday life, research into them is particularly important in an era where concerns about the environment and human health are becoming more widely recognized [27,66,71]. The study not only explores the interactions and toxicity details of BPA and its analogs but also broadens its scope to address wider issues, such as the possible health effects, which have acquired attention worldwide [35]. Unraveling the intricate interactions between these compounds and AR using state-of-the-art methods, including molecular docking, ADMET prediction, MDS, and extensive experimental investigations [82] provides results crucial not only for the scientific community but also for governance, policy-making, and real-world applications [10]. Studies of this kind are crucial as they contribute to the development of policies aimed at protecting human health and the environment by elucidating the potential effects of BPA and its analogs [26,78]. Therefore, the present study aims to fill the knowledge gap between science and practical applications, promoting a holistic strategy for addressing today's challenges.

2. Materials and methods

2.1. Dataset of the three-dimensional (3D) structures of BPA, its analogs, and AR

The three-dimensional (3D) structures of BPA and its analogs (a total of 22 compounds) were obtained from the PubChem database (<https://pubchem.ncbi.nlm.nih.gov/>) in the structure-data file format (SDF) [24]. To prepare these compounds for molecular docking studies, the OpenBabel (https://openbabel.org/wiki/Main_Page) chemical toolbox was used to convert them into PDBQT files. These files include information about the Protein Data Bank (PDB) format, partial charges (Q), and atom types (T). For the receptor, the structure of AR co-crystallized with DHT

(PDB ID: 1T63) was downloaded from the PDB database (<https://www.rcsb.org>) [13]. To ensure accurate docking, the AR structure was visualized and analyzed using UCSF Chimera1.15 [51]. Non-standard residues and the co-crystallized ligand were removed, and a PDBQT file for AR was created using AutoDockTools1.5.6, with added charges and polar hydrogens [15,40]. We defined the grid box size to encompass the binding cavity of the co-crystallized ligand DHT. The grid box size was set to 40 Å in each dimension (x, y, and z), with a grid spacing of 0.375 Å. The coordinates of the center of the grid box were set to -29.698, 31.139, and 5.225 Å, respectively. To validate the docking parameters, we performed redocking experiments using AutoDock Vina, where we redocked the co-crystallized ligand DHT onto its receptor [12, 73]. The accuracy of the docking was evaluated by calculating the root-mean-square deviation (RMSD) between the co-crystallized ligand and its re-docked conformation using the ProRMSD tool [5].

2.2. Molecular docking of BPA and its analogs with AR

To explore the interaction of BPA and its analogs with AR, molecular docking studies were conducted using AutoDock Vina [73]. The co-crystallized ligand DHT was chosen as the reference. Subsequently, UCSF Chimera 1.15 was used to generate protein-ligand complexes for further analysis [51]. To gain insights into the specific interactions contributing to the binding process, both two-dimensional (2D) and 3D diagrams of the protein-ligand interaction were constructed using the Discovery Studio Visualizer 2021 software (<https://discover.3ds.com/discovery-studio-visualizer-download>). These results aid in identifying key amino acid residues involved in the binding process through various types of interactions, including hydrogen and hydrophobic bonding [47].

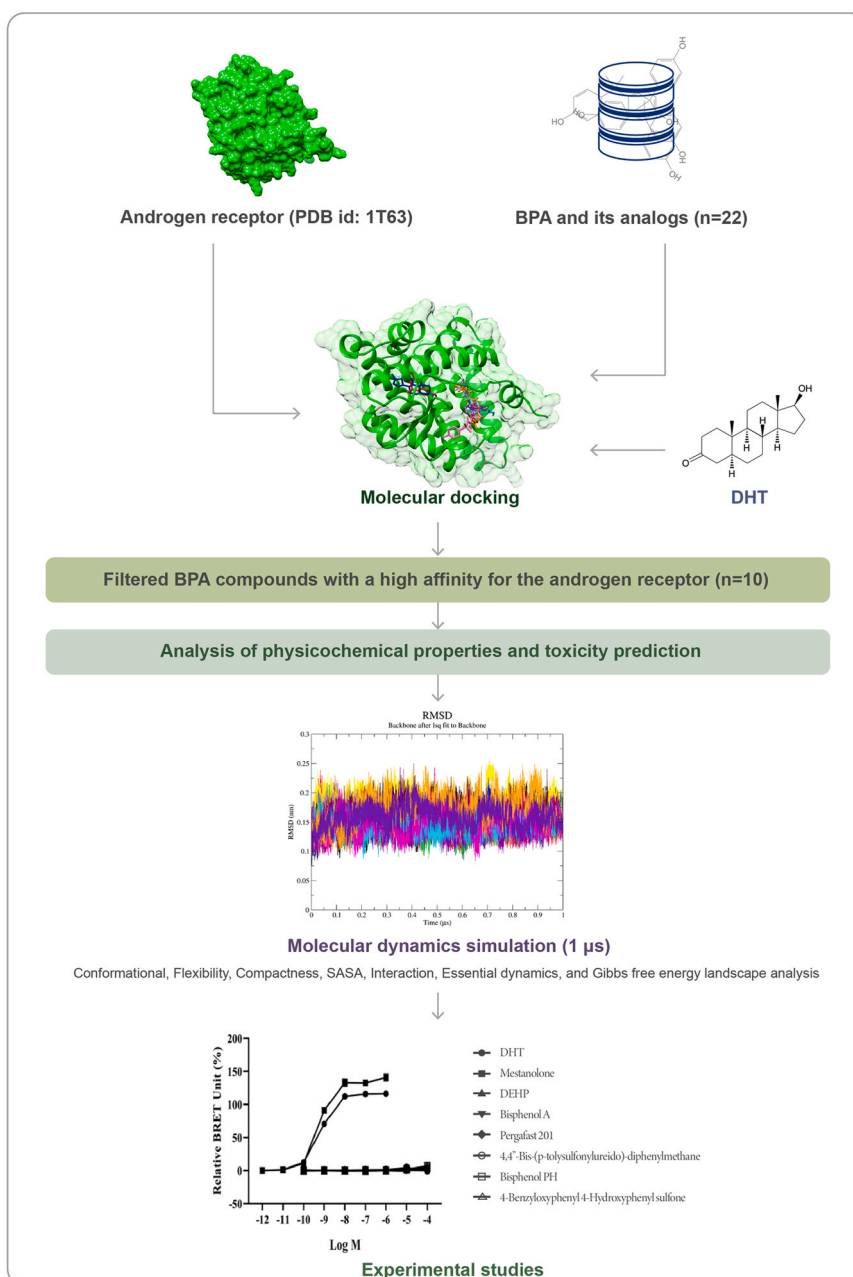


Fig. 1. Summary of work conducted to investigate interactions between bisphenol A (BPA) and its analogs with the androgen receptor (AR).

2.3. Characterization of physicochemical properties and toxicity prediction

Characterization of physicochemical properties and toxicity analyses were performed for the top-10 BPA compounds, along with the reference DHT, which exhibited a stronger binding affinity with AR. Data from the PubChem database (<https://pubchem.ncbi.nlm.nih.gov/>) provided valuable information about each compound's molecular weight, logP, and hydrogen bond (HB) donor and acceptor, as well as their topological surface area. Additionally, the OSIRIS Property Explorer (<https://www.organic-chemistry.org/prog/peo/>) was used to predict the toxic properties of these compounds. This tool utilizes the Registry of Toxic Effects of Chemical Substances (RTECS) database to predict toxicity. The predictive process depends on a precomputed collection of structural fragments. These fragments trigger toxicity alerts when found in the structure currently being examined. The lists of fragments were compiled by analyzing all compounds in the RTECS database known to demonstrate activity in particular toxicity classes (<https://www.organic-chemistry.org/prog/peo/tox.html>). This tool aided in assessing potential mutagenic, tumorigenic, and irritant properties associated with each compound.

2.4. Molecular dynamics simulations (MDS)

The top-10 BPA compound-AR complexes, based on binding free energy, along with the DHT-AR complex and AR, were selected for MDS. The MDS was conducted using the GPU-accelerated GROMACS package version 2018.1, employing the CHARMM27 all-atom force field [45,75]. Ligand topologies were generated using SwissParam [84]. A dodecahedron water box was created and solvated with the TIP3P water model. Counter ions were added to neutralize the system, which was then minimized using the steepest descent minimization algorithm. Subsequently, the system was equilibrated using NVT and NPT to maintain volume, temperature, and pressure [49,57]. The remaining parameters were set as default. All systems underwent a 1 μ s (1000 ns) simulation time. The structural stability of AR and AR-ligand complexes was assessed using RMSD, flexibility was analyzed using root-mean-square fluctuation (RMSF), and compactness was evaluated using the radius of gyration (R_g). Protein folding and stability were examined through solvent-accessible surface area (SASA) analysis, while protein-ligand interactions were studied using HB analysis. Structural motions were analyzed through principal component analysis (PCA) using several GROMACS utilities, including 'gmx,' 'rms,' 'rmsf,' 'gyrate,' 'sasa,' 'hbond,' 'covar,' and 'anaeig.' The 2D plotting program Grace (<https://plasma-gate.weizmann.ac.il/Grace/>) was employed for graphical analysis and visualization. FEL analysis was undertaken to determine the minimum energy states of AR, AR-DHT, and AR-BPA compound complexes. The FEL was calculated using the 'gmxsham' GROMACS utility (<https://www.gromacs.org/>).

2.5. Experimental analyses

2.5.1. Chemicals

The reference substrates 5 α -DHT (DHT, CASRN 521-18-6), mestanolone (CASRN 521-11-9), bicalutamide (CASRN 90357-06-5), bis(2-ethylhexyl)phthalate (DEHP, 117-81-7), and BPA (80-05-7) for the BRET-based AR dimerization confirmation assay were commercially purchased (Table S1). The stock concentration and exposure range of each test substrate were determined according to the AR dimerization assay included in the OECD AOP26 [29].

2.5.2. Confirmation of AR dimerization in cytosol using BRET-based assay

The substrate-induced cytosolic AR homodimerization was assessed using an in vitro BRET-based assay [29]. HEK293 cells, which were stably co-transfected by cloning a full sequence of an AR to the pFC31A Nluc CMV-Hygro Flexi® vector and the pFN27AHaloTag® CMV-neo

Flexi® vector, were obtained from routinely maintained in a 5% CO₂ atmosphere at 37 °C in MEM supplemented with 10% FBS, 100 U/mL penicillin-streptomycin, 100 μ g/mL hygromycin B, and 400 μ g/mL G418. For the NanoBRET-based AR dimerization assay, cells (with or without 100 nMHaloTag® protein [HaloTag®NanoBRET™ 618 Ligand]) were seeded at a density of 2.2×10^5 cells/mL in test medium (MEM supplemented with 4% DCC-FBS, 100 μ g/mL hygromycin B, and 400 μ g/mL G418) and were incubated for 1 h at 37 °C in a 5% CO₂ atmosphere. Afterward, cells were treated with 10 μ L of the prepared chemicals at the concentration range of 10^{-4} – 10^{-7} M, determined by a solubility test using DMSO in accordance with the optimized protocol in our previous study [29], and incubated at 37 °C in a 5% CO₂ atmosphere for 24 h. Vehicle control (VC) and positive control (PC) wells contained 0.1% DMSO and 10 n MDHT, respectively. To determine inducing AR dimerization in the cytosol via binding to AR, 2.5 mL of test medium was mixed with 25 μ L of NanoBRET™ NanoBRET® substrate reagent (Promega, WI, USA), and the mixture was added to the assay plates (25 μ L/well). The bioluminescence and fluorescence were measured using the GloMax® multiplate reader within 10 min. For the cell viability, 125 μ L of CellTiter-Glo® 2.0 Cell Viability Assay reagent (Promega) was added directly to the assay wells after the binding affinity, and the 96-well plate was blocked from light and left for 30 min. The luminescence was measured using a GloMax® multiplate reader. For the BRET-based AR dimerization assay, data transformations to relative BRET units (RLU) were performed as follows:

$$\text{Raw BRET unit} = \frac{\text{RLU value of acceptor(HT)}}{\text{RLU value of donor(Nluc)}}$$

Raw BRET units were generated to evaluate dimerization affinity by comparing the test chemical to the PC as follows:

$$\text{Relative BRET unit(\%)} = \frac{\text{Mean} - \text{corrected BRET unit of test substance}}{\text{Mean} - \text{corrected BRET unit of PC}} \times 100$$

The criterion for data interpretation was as follows: If the maximal activity of the test chemical is equal to or exceeds 10% of the response of the PC (10nMDHT), in the absence of cytotoxicity, it is determined to have AR binding affinity.

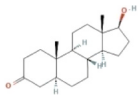
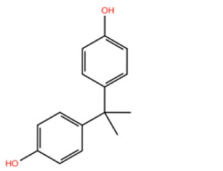
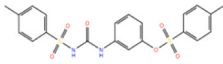
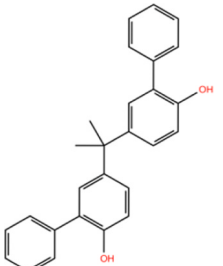
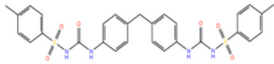
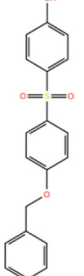
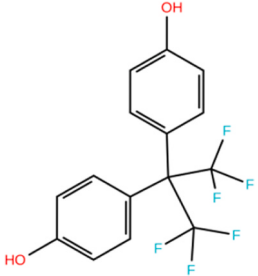
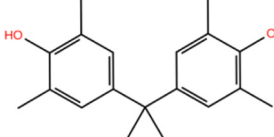
3. Results

3.1. Molecular docking for quantifying the binding energy of BPA and its analogs with AR compared to DHT

Molecular docking enables the exploration of optimal intermolecular interactions between macromolecular targets and ligands, allowing for the identification of the most favorable binding interactions and the prediction of their potential to form a complex. This provides valuable insights into the strength of the interactions between the target and ligand by assessing the binding energy obtained during molecular docking. In the present study, we calculated the binding energy of the co-crystallized DHT with AR to understand how well BPA and its analogs interacted. The binding energy of the co-crystallized ligand DHT was – 11.0 kcal/mol, and the RMSD value between DHT and its re-docked conformation was predicted to be 0.565 Å. This serves as an important measure of the efficiency and accuracy of the docking protocol. Generally, when a ligand exhibits low binding energy with its target, its binding affinity is considered stronger. Therefore, the top-10 BPA analogs, including BPA, which showed the lowest binding energy with AR, were chosen for further investigation, along with DHT as a reference. Table 1 lists the names of BPA compounds along with the reference compound DHT, their 2D structure, PubChem ID, Chemical Abstracts Service (CAS) registry number, binding free energy, and the specific amino acids involved in their interactions.

Table 1

Binding energy of DHT, BPA, and BPA structural analogs with AR along with their 2D structure, PubChem ID, CAS, interacting amino acid residues, and type of interaction.

S.N.	Compound name	2D structure	PubChem ID	CAS	Binding energy (kcal/mol)	Interacting amino acid residues	Type of interactions
1.	DHT (Reference)		10635	521-18-6	- 11.0	Leu704, Arg752, Phe764, Met780, Leu873, Thr877	Conventional hydrogen bond, alkyl, pi-alkyl
2.	Bisphenol A (BPA)		6623	80-05-7	- 8.6	Leu704, Asn705, Gln711, Met745, Met749, Phe764, Met895	Conventional hydrogen bond, carbon-hydrogen bond, unfavorable acceptor-acceptor, pi-sulfur, pi-pi T-shaped, amide-pi stacked, pi-alkyl
3.	3-(3-(Tosylureido)phenyl p-toluenesulfonate (Pergafast 201)		22035425	232938-43-1	- 10.2	Pro682, Gly683, Val684, Val715, Leu744, Ala748, Arg752, Asn756, Pro766, Lys808	Conventional hydrogen bond, pi-donor hydrogen bond, alkyl, pi-alkyl
4.	2,2-Bis(2-hydroxy-5-biphenyl) propane (Bisphenol PH, BPPH)		13059052	24038-68-4	- 9.8	Pro682, Val684, Val715, Trp718, Leu744, Ala748, Arg752, Lys808	Pi-cation, pi-sigma, pi-pi T-shaped, pi-alkyl
5.	Benzenesulfonamide, N,N'-(methylenebis(4,1-phenyleneiminocarbonyl))bis(4-methyl (BTUM) or 4,4'-Bis-(p-tolylsulfonyleureido)-diphenylmethane		3596056	151882-81-4	- 9.6	Pro682, Val684, Val715, Trp718, Leu744, Ala748, Arg752, Val757, Tyr763, Val769, Lys808	Conventional hydrogen bond, carbon-hydrogen bond, pi-sigma, pi-pi T-shaped, alkyl, pi-alkyl
6.	4-((4-(Benzyloxy)phenyl) sulfonyl)phenol (BPSP) or 4-Benzyloxyphenyl 4-hydroxyphenyl sulfone		113063	63134-33-8	- 8.7	Glu681, Pro682, Val715, Trp718, Leu744, Ala748, Trp751, Arg752, Lys808	Carbon-hydrogen bond, pi-cation, pi-anion, pi-sigma, pi-sulfur, pi-pi T-shaped, pi-alkyl
7.	Bisphenol AF (BPAF)		73864	1478-61-1	- 8.5	Leu704, Leu707, Gln711, Trp741, Met742, Arg752, Phe764, Leu873, Met895	Conventional hydrogen bond, pi-sulfur, pi-pi T-shaped, alkyl, pi-alkyl
8.	2,2-Bis(4-hydroxy-3,5-dimethylphenyl)propane (Bisxylenol A, BXA)		79717	5613-46-7	- 8.5	Leu701, Leu704, Asn705, Gln711, Phe764, Met787, Thr877, Leu880	Conventional hydrogen bond, pi-sulfur, pi-pi T-shaped, alkyl, pi-alkyl

(continued on next page)

Table 1 (continued)

S.N.	Compound name	2D structure	PubChem ID	CAS	Binding energy (kcal/mol)	Interacting amino acid residues	Type of interactions
9.	Bisphenol E (BPE)		608116	2081-08-5	- 8.4	Leu704, Asn705, Met745, Met749, Phe764, Met895	Carbon-hydrogen bond, pi-sulfur, pi-pi T-shaped, amide-pi stacked, pi-alkyl
10.	2,2-Bis(4-hydroxy-3-methylphenyl)propane or Bis-o-cresol A		6620	79-97-0	- 8.4	Leu704, Asn705, Leu707, Gln711, Met742, Trp741, Phe764, Thr877	Conventional hydrogen bond, pi-pi T-shaped, alkyl, pi-alkyl
11.	Methyl bis(4-hydroxyphenyl)acetate (MBHA)		78805	5129-00-0	- 8.3	Leu704, Asn705, Gln711, Met745, Met749, Arg752, Phe764, Met895	Conventional hydrogen bond, carbon-hydrogen bond, unfavorable donor-donor, pi-sulfur, pi-pi T-shaped, pi-alkyl
12.	Bisphenol P (BPP)		630355	2167-51-3	- 8.3	Pro682, Val715, Trp718, Ala748, Arg752, Asn756, Lys808	Unfavorable donor-donor, pi-cation, pi-sigma, pi-pi T-shaped, pi-alkyl
13.	Bisphenol A bis(diphenyl phosphate)		9874825	5945-33-5	- 8.2	Glu681, Pro682, Val684, Val685, Ala748, Arg752, Tyr763, Pro766	Attractive charge, conventional hydrogen bond, unfavorable positive-positive, pi-cation, pi-donor hydrogen bond, pi-sigma, pi-pi T-shaped, pi-alkyl
14.	Bisphenol Z (BPZ)		232446	843-55-0	- 8.1	Leu704, Met745, Phe764, Leu873, Met895	Conventional hydrogen bond, sulfur-X, pi-sulfur, pi-pi T-shaped, alkyl, pi-alkyl
15.	Bisphenol B (BPB)		66166	77-40-7	- 8.0	Leu704, Asn705, Gln711, Met742, Met745, Met749, Arg752, Phe764, Leu873, Met895	Conventional hydrogen bond, unfavorable donor-donor, pi-sulfur, pi-pi T-shaped, amide-pi stacked, alkyl, pi-alkyl
16.	Bisphenol F (BPF)		12111	620-92-8	- 8.0	Leu704, Asn705, Gln711, Met745, Met749, Phe764, Met895	Conventional hydrogen bond, pi-sulfur, pi-pi T-shaped, amide-pi stacked, pi-alkyl

(continued on next page)

Table 1 (continued)

S.N.	Compound name	2D structure	PubChem ID	CAS	Binding energy (kcal/mol)	Interacting amino acid residues	Type of interactions
17.	2,4'-Dihydroxydiphenyl sulfone (2,4-BPS)		79381	5397-34-2	- 7.8	Pro682, Gly683, Val715, Trp718, Leu744, Met745, Ala748, Arg752, Lys808	Conventional hydrogen bond, carbon-hydrogen bond, pi-cation, pi-sigma, pi-pi T-shaped, pi-alkyl
18.	2,2'-Bisphenol F(2,2'-BPF)		75575	2467-02-9	- 7.8	Pro682, Val715, Trp718, Leu744, Met745, Ala748, Arg752, Lys808	Carbon-hydrogen bond, pi-cation, pi-sigma, pi-pi T-shaped, pi-alkyl
19.	Phenol, 4,4'-sulfonylbis[2-(2-propenyl)]		833466	41481-66-7	- 7.5	Leu701, Leu704, Asn705, Gly708, Met745, Val746, Met749, Phe764, Met780, Met787, Leu873, Met895	Conventional hydrogen bond, carbon-hydrogen bond, pi-sulfur, pi-pi T-shaped, alkyl, pi-alkyl
20.	4-((4-Allyloxy)phenyl)sulfonyl phenol		2054598	97042-18-7	- 7.4	Leu704, Leu707, Gln711, Trp741, Met745, Met749, Arg752, Phe764, Met780, Phe876	Conventional hydrogen bond, unfavorable acceptor-acceptor, pi-sulfur, pi-pi T-shaped, alkyl, pi-alkyl
21.	Bisphenol AP (BPAP)		623849	1571-75-1	- 6.7	Phe876, Asp879, Leu880, Lys883	Pi-cation, pi-anion, pi-pi stacked, pi-pi T-shaped, pi-alkyl
22.	4-((4-Isopropoxyphenyl)sulfonyl)phenol		9904141	95235-30-6	- 6.7	Glu678, Glu681, Pro682, Ala748, Trp751, Arg752	Conventional hydrogen bond, pi-anion, pi-sulfur, alkyl, pi-alkyl
23.	Bis[2-(4-hydroxyphenylthio)ethoxy]methane		3086375	93589-69-6	- 6.6	Leu704, Trp741, Met742, Met780, Thr877, Met895	Conventional hydrogen bond, pi-sulfur, pi-pi T-shaped, pi-alkyl

3.2. Structural visualization and analysis of docked complexes of DHT, BPA, and their top-screened analogs with AR

After analyzing the binding energy, it is crucial to examine protein-ligand interactions. Among the 22 BPA analogs, the top 10 were selected, including BPA itself (binding energy range: -10.2 to -8.3 kcal/mol), along with DHT (-11.0 kcal/mol), to determine their interactions with AR. The binding site area of the co-crystallized ligand, DHT, was targeted during molecular docking. It was predicted that the binding characteristics of DHT and BPA were similar, whereas the top-screened BPA analogs showed a relatively higher affinity with AR in terms of binding energy bound to different regions on AR (Fig. 2). To gain further insights into the interaction between these molecules and the receptor, the same approach was used to assess the bonds formed between the target and the ligand, which play a crucial role in the interaction. The reference compound DHT was found to form two conventional HBs with Arg752 and Thr877, in addition to five pi-alkyl bonds with the amino acid residues Leu704, Phe764, Met780, and Leu873 (Figs. 3A and 3B). BPA was found to interact with AR at amino acid residues Asn705, Gln711, and Met745 through one carbon-hydrogen bond and two conventional HBs. Amino acid residues Leu704 and Phe764 interacted through pi-pi T-shaped and amide-pi stacked bonds, whereas Met745 and Met749 interacted through two pi-alkyl bonds. Additionally, Met895 interacted through one pi-sulfur bond. The binding energy between AR and BPA was predicted to be -8.6 kcal/mol (Figs. 3C and 3D).

Pergafast201 interacts with Pro682, Gly683, and Arg752 through five conventional HBs; Asn756 is involved in the interaction through one pi-donor HB. Val684, Val715, Leu744, Ala748, Pro766, and Lys808 contribute to the interaction through six alkyl bonds and three pi-alkyl

bonds, resulting in a binding energy of -10.2 kcal/mol (Fig. 4A). Bisphenol PH (BPPH) interacts with Pro682, Ala748, and Leu744 through five pi-alkyl bonds; Val684 and Val715 form two pi-sigma bonds; Arg752 forms one pi-alkyl and one pi-cation bond, and Lys808 forms one pi-cation bond. Additionally, Trp718 forms one pi-pi T-shaped bond, resulting in a binding energy between AR and BPPH of -9.8 kcal/mol (Fig. 4B). Benzenesulfonamide, *N,N'*-(methylenebis(4,1-phenyleneiminocarbonyl)) bis (4-methyl (BTUM) interacts with Pro682 through one conventional HB and pi-alkyl bond. Arg752 participates in the interaction through one conventional HB, one carbon-hydrogen bond, and one pi-alkyl bond. This amino acid forms alkyl bonds with Val757, Tyr763, and Val769. Amino acid residues Val684 and Val715 contribute to the interaction through a pi-sigma bond, and Trp718 interacts through pi-pi T-shaped and pi-sigma bonding. Leu744 is involved in the interaction through alkyl bonding, Ala748 forms pi-alkyl bonding, and Lys808 participates in the interaction through alkyl and pi-alkyl bonding. The resulting binding energy of AR with BTUM is -9.6 kcal/mol (Fig. 4C). With 4-((4-(benzyloxy)phenyl)sulfonyl)phenol (BPSP), one carbon-hydrogen and one pi-sulfur bond are formed with Trp751; three amino acid residues (Glu681, Arg752, and Lys808) are involved in pi-anion and pi-cation interactions; Pro682, Leu744, and Ala748 form five pi-alkyl bonds; and Val715 and Trp718 contribute to the interaction through pi-sigma and pi-pi T-shaped bonding, respectively. The binding energy between AR and BPSP is predicted to be -8.7 kcal/mol (Fig. 4D). BPAF interacts with Gln711 and Arg752 through three conventional HBs; Leu704 and Met742 form one alkyl bond and one pi-alkyl bond; Leu707 forms a pi-alkyl bond; and Leu873 forms an alkyl bond. Trp741 and Phe764 participate in the interaction through pi-pi T-shaped bonding, and Met895 forms a pi-sulfur bond, resulting in a binding energy of -8.5 kcal/mol (Fig. 4E). Bisxylenol A (BXA) interacts with

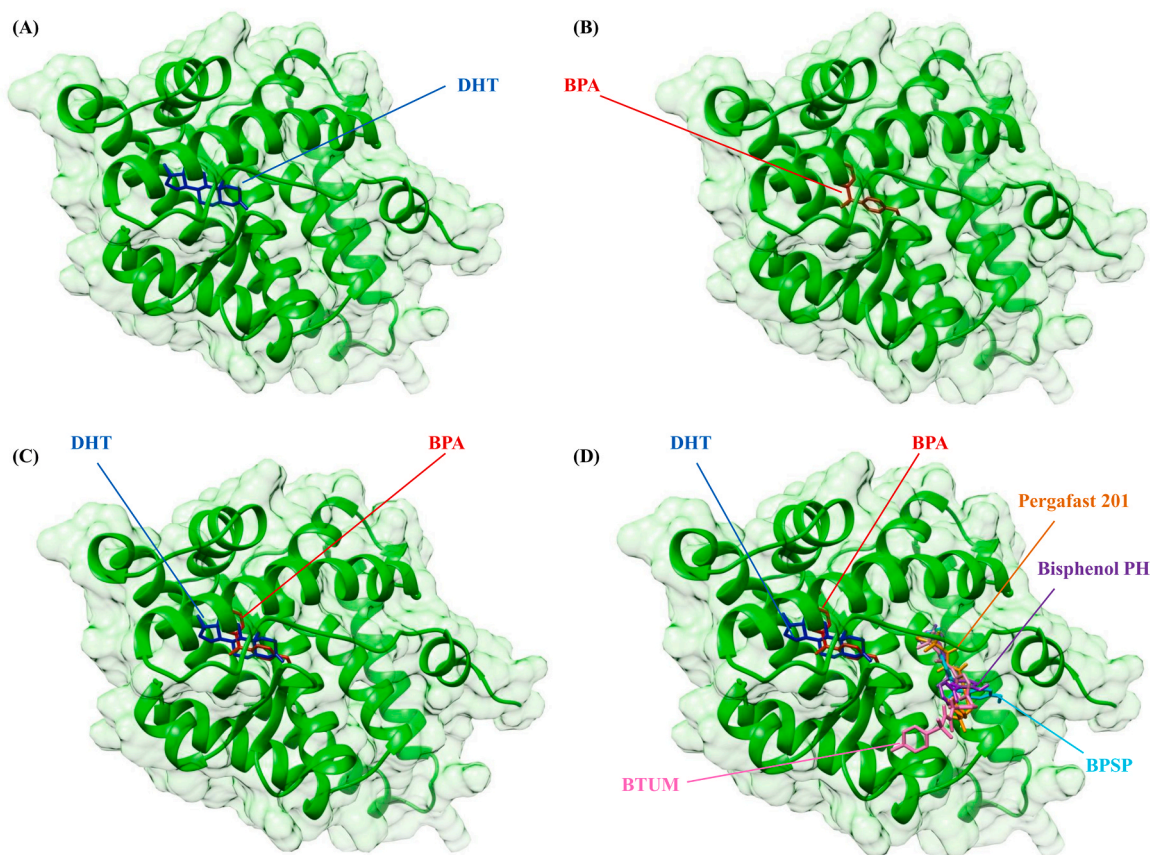


Fig. 2. Binding characteristics of BPA and its top-screened analogs compared to DHT with AR. The figure illustrates the binding of BPA to the same regions where DHT binds, while the interactions of other BPA analogs differ from BPA. (A) DHT interaction with AR. (B) BPA interaction with AR. (C) Interaction of DHT and BPA with AR. (D) Interaction of BPA and its top-screened analogs (Pergafast 201, BPPH, BTUM, and BPSP) with AR compared to DHT.

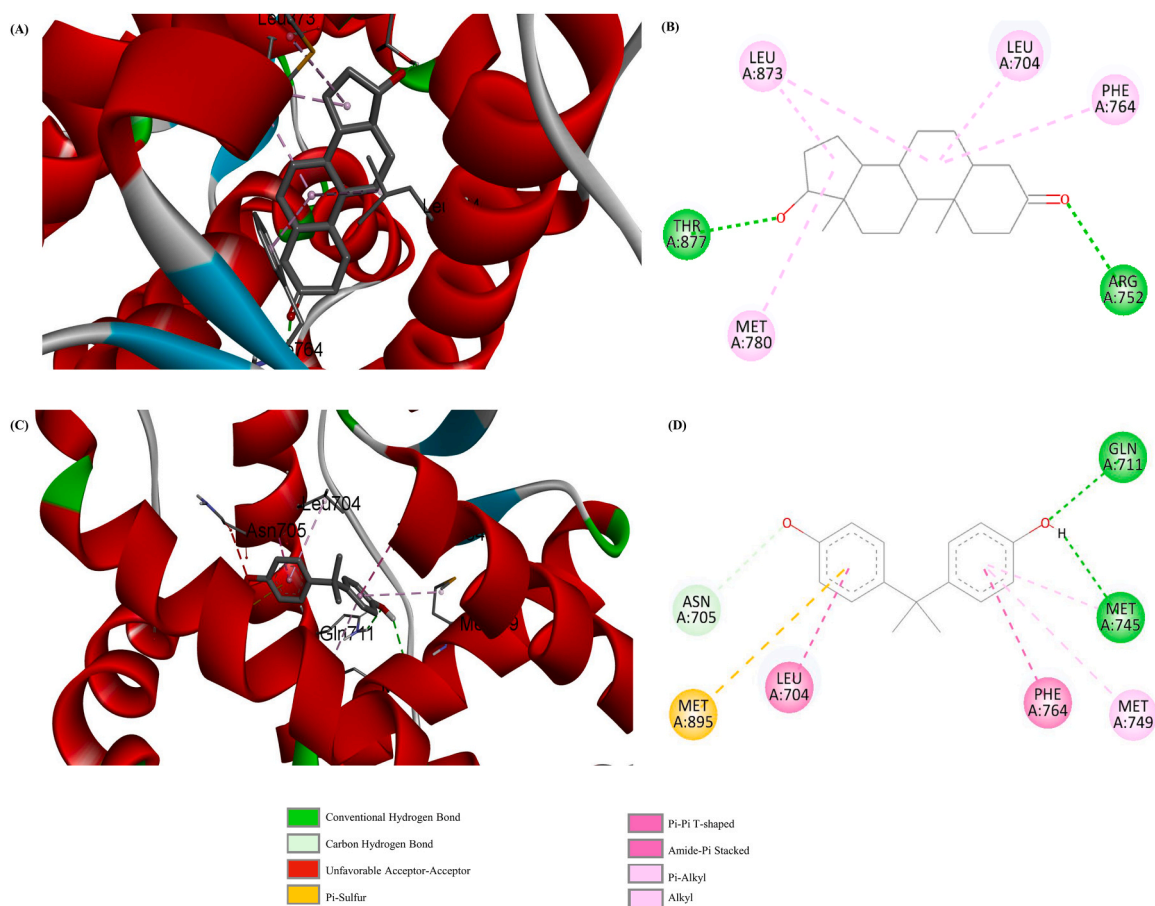


Fig. 3. Three-dimensional and two-dimensional representations of the binding interactions of the reference compound DHT and BPA with AR, highlighting key amino acid residues that contribute to the protein-ligand interactions; **(A and B)** DHT and **(C and D)** BPA.

Asn705, Gln711, and Thr877 through conventional HBs. Leu701 and Leu880 form an alkyl bond, Leu704 participates in the interaction through pi-alkyl bonding, and Phe764 and Met787 are involved in the interaction through pi-pi T-shaped and pi-sulfur bonds. The binding energy between BXA and AR is predicted to be -8.5 kcal/mol (Fig. 4F). Bisphenol E (BPE) interacts with Asn705 through a carbon-hydrogen bond, and with Leu704 and Phe764 through pi-pi T-shaped bonding. It interacts with Met745 and Met749 through a pi-alkyl bond. It forms a pi-sulfur bond with Met895. The binding energy is predicted to be -8.4 kcal/mol (Fig. 4G). Bis-*o*-cresol A interacts with Asn705, Gln711, and Thr877 through conventional HBs and forms two and one pi-alkyl bond with Leu704 and Leu707, respectively. Trp741 and Met742 participate in the interaction through alkyl bonds, whereas Phe764 forms one pi-pi T-shaped bond. The binding energy between AR and Bis-*o*-cresol A is predicted to be -8.4 kcal/mol (Fig. 4H). Methyl bis(4-hydroxyphenyl) acetate (MBHA) interacts with Arg752 through conventional HB. It interacts with Leu704 and Phe764 through pi-pi T-shaped and amide-pi stacked bonds. Met745 and Met749 form pi-alkyl bonds, and Met895 participates in the interaction through a pi-sulfur bond. Gln711 forms an unfavorable donor-donor bond. The binding energy between MBHA and AR is predicted to be -8.3 kcal/mol (Fig. 4I).

3.3. Evaluation of physicochemical properties and toxicity profile of BPA and its analogs

The physicochemical properties of BPA and the BPA analogs exhibiting higher affinity with AR were evaluated and compared to those of DHT as the reference. We focused on eight key principal descriptors, including molecular weight, logP, HB donor, HB acceptor, topological

polar surface area, mutagenic, tumorigenic, and irritant properties. Physicochemical properties were retrieved from the PubChem database, and toxicity was predicted by the OSIRIS Property Explorer. In the present study, most BPA analogs adhered to Lipinski's rule of five, indicating drug-like properties. However, three compounds, namely BXA with a logP value of 5.5, BPPH with a logP value of 7.3, and BTUM with a molecular weight of 592.7, and logP value of 6.1, deviated from this pattern. These compounds exhibited characteristics similar to orally administered drugs, suggesting easy absorbability by both humans and animals. Additionally, these compounds had polar surface areas smaller than 140 \AA^2 , implying that they could easily pass through cell membranes, except for BTUM. Regarding toxicity prediction, BPA and its analog Bis-*o*-cresol were found to have mutagenic, tumorigenic, and irritant effects. BTUM demonstrated mutagenic and tumorigenic properties. Furthermore, most of the top-10 selected BPA analogs were predicted to have irritant properties, except for Pergafast 201, BTUM, and MBHA. Detailed results from the analysis of both the physicochemical properties and toxicity are listed in Table 2.

3.4. Comparative MDS and structural conformational analysis of unbound and bound states of AR

MDS was conducted to elucidate the dynamic behaviors of AR in its unbound state and upon binding with the reference DHT and BPA analogs. Various key parameters were studied to comprehensively summarize the outcomes, including RMSD, RMSF, R_g , SASA, HB interactions, PCA, and FEL analysis.

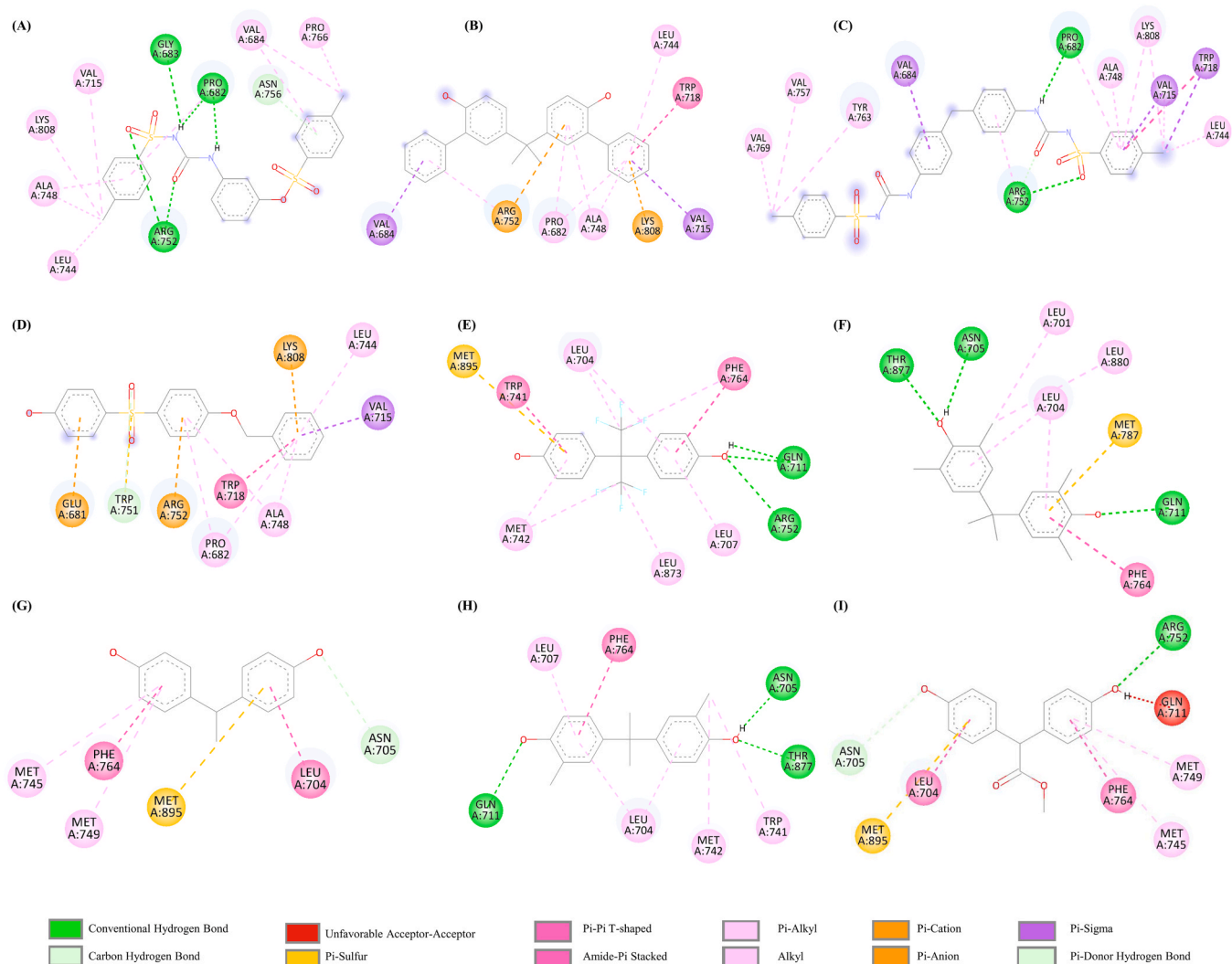


Fig. 4. Two-dimensional representations of the binding interactions of the BPA analogs with AR, highlighting key amino acid residues that contribute to the protein-ligand interactions. (A) Pergafast 201, (B) BPPH, (C) BTUM, (D) BPSp, (E) BPAF, (F) BXA, (G) BPE, (H) Bis-*o*-cresol A, and (I) MBHA.

Table 2

Physicochemical properties and toxicity-related characteristics of DHT, BPA, and selected BPA analogs. BPA analogs are ranked according to their binding free energy with AR.

S.N.	Compound name	PubChem ID	MW (g/mol)	LogP	HB donor	HB acceptor	TPSA (Å ²)	Mutagenic	Tumorigenic	Irritant
1.	DHT (Reference ligand)	10635	290.4	3.7	1	2	37.3	No	No	No
2.	Bisphenol A (BPA)	6623	228.29	3.3	2	2	40.5	Yes	Yes	Yes
3.	3-(3-Tosylureido)phenyl <i>p</i> -toluenesulfonate (Pergafast 201)	22035425	460.5	4.6	2	6	135	No	No	No
4.	2,2-Bis(2-hydroxy-5-biphenyl)propane (Bisphenol PH, BPPH)	13059052	380.5	7.3	2	2	40.5	No	No	Yes
5.	Benzenesulfonamide, <i>N,N'</i> -(methylenebis(4,1-phenyleneimino-carbonyl))bis(4-methyl (BTUM) or 4,4''-Bis-(<i>p</i> -tolylsulfonylureido)-diphenylmethane	3596056	592.7	6.1	4	6	167	Yes	Yes	No
6.	4-((4-(Benzyloxy)phenyl)sulfonyl)phenol (BPSp) or 4-Benzyloxyphenyl 4-hydroxyphenyl sulfone	113063	340.4	4.2	1	4	72	No	No	Yes
7.	Bisphenol AF (BPAF)	73864	336.23	4.5	2	8	40.5	No	No	Yes
8.	2,2-Bis(4-hydroxy-3,5-dimethylphenyl)propane (Bisxylenol A, BXA)	79717	284.4	5.5	2	2	40.5	No	No	Yes
9.	Bisphenol E (BPE)	608116	214.26	3.9	2	3	40.5	No	No	Yes
10.	2,2-Bis(4-hydroxy-3-methylphenyl)propane or Bis- <i>o</i> -cresol A	6620	256.34	4.7	2	2	40.5	Yes	Yes	Yes
11.	Methyl bis(4-hydroxyphenyl)acetate (MBHA)	78805	258.27	2.7	2	4	66.8	No	No	No

Mw: molecular weight; TPSA: topological polar surface area.

3.4.1. Conformational stability analysis

The stability of AR was assessed through the RMSD analysis of the MDS trajectory, where a lower RMSD indicates a more stable structure. RMSD was measured over 1000 ns (1 μ s) to understand structural deviations over time. AR, as well as all selected docked complexes, exhibited low RMSD values based on the RMSD plot of backbone C-alpha atoms. The average RMSD of AR was calculated as 0.15 nm. This same value was determined for the AR-MBHA complex. It was relatively lower for six of the remaining complexes, which all had an RMSD of 0.14 nm. Only the AR-BPSP, AR-Pergafast 201, AR-Bis-*o*-cresol A, and AR-BPPH complexes had comparatively higher RMSD values, at 0.16, 0.16, 0.17, and 0.17 nm, respectively. These data suggest that AR-DHT, AR-BPA, AR-BTUM, AR-BPAF, AR-BXA, and AR-BPE, with lower RMSD values, form more stable complexes relative to the others. However, throughout the simulation, all systems appeared to be well-equilibrated and formed stable complexes (Fig. 5A).

3.4.2. Flexibility and residual mobility analysis

The results of RMSF analyses provided valuable insights into the flexibility and mobility of protein amino acid residues. In this study, the RMSF of AR and AR-ligand complexes were investigated over a duration of 1 μ s. The average RMSF of AR was calculated as 0.08 nm, and this same value was calculated for the AR-BPA, AR-BPAF, AR-BPE, AR-BTUM, AR-MBHA complexes. A slightly lower 0.07 nm was determined for the AR-BXA and AR-DHT complexes, whereas the AR-Bis-*o*-cresol A, AR-BPPH, AR-BPSP, and AR-Pergafast 201 complexes had a

marginally higher RMSF of 0.09 nm, respectively. Higher RMSF values were observed due to ligand binding leading to alterations in AR geometry (Fig. 5B).

3.4.3. Compactness analysis

Changes in protein structure, stability, and folding over time can be characterized by calculating the R_g values. These values are indicative of structural compactness; therefore, R_g values were determined for AR and its complexes. The average R_g of AR was calculated as 1.81 nm. Only AR-Bis-*o*-cresol A, AR-BXA, and AR-Pergafast 201 had an R_g different from this value, being slightly higher at 1.82 nm. It can be inferred from these results that the structure of these three complexes is less compact than the others (Fig. 5C).

3.4.4. Solvent-accessible surface area (SASA) analysis

SASA analysis throughout the 1 μ s simulation duration was conducted to evaluate the influence of the ligand on the SASA. The average SASA for AR was calculated as 127.14 nm², whereas the SASA for the AR-BTUM, AR-BPA, AR-MBHA, AR-BPSP, AR-BPAF, AR-DHT, AR-BPPH, AR-Bis-*o*-cresol A, AR-BPE, AR-Pergafast 201, and AR-BXA complexes were 126.10, 126.92, 127.37, 127.39, 127.40, 127.50, 127.64, 128.41, 129.03, 129.14, and 129.16 nm², respectively. The SASA for the AR-BPE, AR-Pergafast 201, and AR-BXA complexes were higher than that for AR-DHT and other complexes. A consistent pattern was observed across all the systems studied, as depicted in Fig. 5D. This suggests minimal alterations in the system upon binding of BPA and its

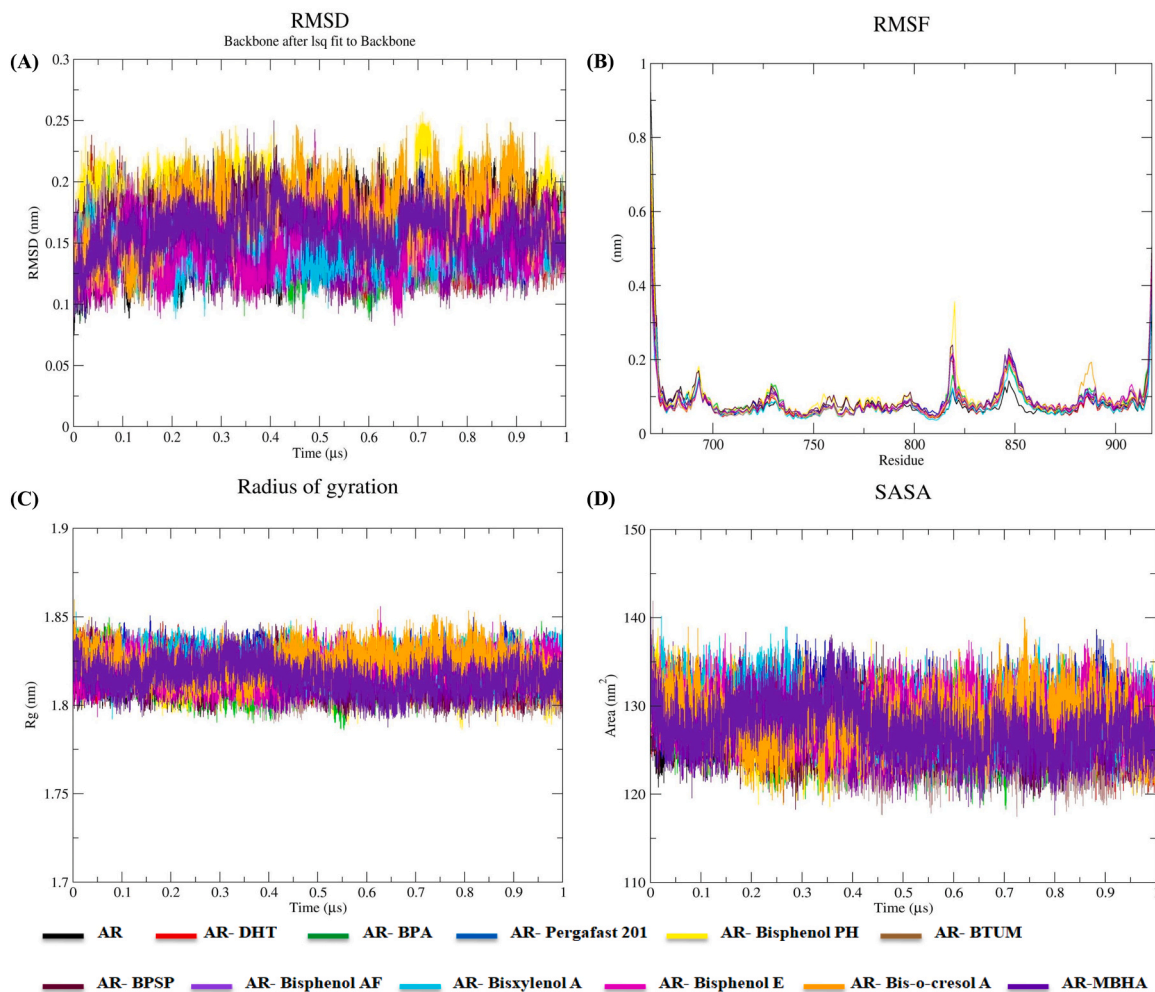


Fig. 5. Stability analysis: (A) RMSD for AR, AR-DHT, and AR-BPA complexes. Flexibility analysis: (B) RMSF for AR, AR-DHT, and AR-BPA complexes. Compactness: (C) R_g and (D) SASA analysis values over 1 μ s of simulations.

analogs.

3.4.5. Interaction analysis

HBs play a crucial role in stabilizing interactions between proteins and ligands. To comprehensively assess these interactions, we conducted an analysis of hydrogen bonding over a 1 μ s period. The AR–DHT complex exhibited 0–4 HBs. This same value was calculated for almost all of the other complexes, differing only for AR–BPE, AR–BTUM, and AR–Pergafast 201, which showed 0–5, 0–7, and 0–10 HBs, respectively. Based on these results, BPE, BTUM, and Pergafast 201 formed more HBs compared to BPA and its other analogs, as well as DHT. However, all the hazardous chemicals exhibited comparable patterns and maintained continuous HBs similar to DHT. This observation indicates a stable nature of interactions between these BPA analogs and the binding cavity of AR (Fig. 6).

3.4.6. Essential dynamics analysis

PCA was conducted to identify significant structural alterations when a ligand binds to the protein. Typically, the initial eigenvectors primarily dictate the entire protein's motion. Therefore, we selected the first 50 eigenvectors to investigate shifts in structural dynamics. To gain precise insights into the motions triggered by ligand binding, we computed correlated motions as percentages from the first five eigenvectors. The first five eigenvectors accounted for 73.55% of the motion for AR. However, the AR–BXA, AR–Bis-*o*-cresol A, AR–MBHA, AR–DHT, AR–BPE, AR–BPSP, AR–BTUM, AR–Pergafast 201, AR–BPA, AR–BPPH, and AR–BPAF complexes exhibited motion correlations of 58.04%, 59.68%, 60.00%, 60.22%, 60.38%, 60.95%, 61.05%, 63.00%, 63.51%, 66.24%, and 68.88%, respectively. Here, we observed that the AR–BXA and AR–Bis-*o*-cresol A complexes exhibited the lowest motions compared to AR–DHT (Fig. 7A). The initial eigenvectors of the protein capture its fundamental dynamics. Consequently, we selected and visualized the first two of these eigenvectors in a phase space and found stable clusters for all the complexes (Fig. 7B).

3.4.7. Gibbs free energy landscape (FEL) analysis

Gibbs FEL was calculated based on the first two principal components (PC1 and PC2). Fig. 8 depicts the FEL for each system; the blue color signifies the conformational state with the lowest energy (kJ mol^{-1}), and red indicates the one with the highest energy (kJ mol^{-1}). Energy values ranging from 0 to 18.1 (AR–BPSP), 18.3 (AR–Bis-*o*-cresol A), 18.7

(AR–BPE), 18.7 (AR–Pergafast 201), 19.1 (AR), 19.1 (AR–BPPH), 19.3 (AR–BPA), 19.5 (AR–BPAF), 19.7 (AR–BXA), 20.3 (AR–MBHA) 21.0 (AR–BTUM), and 21.7 (AR–DHT) were observed. Slight variations in the energy levels of all systems could be seen, except for the AR–BPSP, AR–Bis-*o*-cresol A, AR–BPE, and AR–Pergafast 201 complexes, which displayed marginally lower values than the others. Comparing the FEL values of the AR–DHT complex (0–21.7 kJ mol^{-1}) and the AR–BPA complex (0–19.3 kJ mol^{-1}), as well as its analog complexes, reveals that BPA and its analogs form a more stable complex with AR compared to the reference ligand DHT. Throughout the simulation, these compounds followed the energetically favorable transitions.

3.5. Ligand-mediated homodimerization

The responses of the reference substrates were in line with the anticipated reactions, and the two positive controls (DHT and mestanolone) displayed AR dimerization signals, as indicated by the log PC₁₀ and log PC₅₀ values. The log concentration of the test substrates inducing an effect equivalent to that of a 10% effect on the positive control (log PC₁₀) is representative, and it is used to determine the relative potency of an AR dimerization inducer. These log PC₁₀ values can be calculated by a simple linear regression using two variable data points compared to that of the positive control (10 nMDHT). In the experimental group, BPA and its four analogs did not trigger cytosolic AR dimerization at non-cytotoxic concentrations (cell viability \geq 80.0%) (Fig. 9).

To provide experimental evidence that the docking site of BPA to AR is different from its four analogs by computational modeling prediction, we confirmed the suppressing effect of BPA and its four analogs on androgen-induced AR dimerization through competing reaction in the cytosol according to OECD TG No.458, with a minor modification. The suppressing effect of test substrates on androgen-induced AR dimerization was decided by the criterion used for the classification of an AR antagonist, which is that it has to be able to inhibit the response of 800 pMDHT by at least 30% (IC₃₀). The log IC₃₀ values can also be calculated by a simple linear regression using two variable data points compared to that of the positive control (800 pMDHT). When assessing the interactions between bisphenols and AR in the presence of 800 pMDHT, BPA, and the AR-specific antagonist bicalutamide, we observed that bicalutamide suppressed DHT-induced AR dimerization in the cytosol at non-toxic concentrations, with log IC₃₀ values of $-5.48 \log \text{M}$ and $-6.38 \log \text{M}$, respectively. In contrast, four BPA analogs exhibited no inhibitory effect against DHT-induced cytosolic AR dimerization (Fig. 10).

4. Discussion

BPA, a well-known endocrine disruptor linked to reproductive toxicity, even at very small doses [81]), has been associated with adverse effects on spermatogenesis and sperm attributes, suggesting its potential for male infertility [16]. Exposure to BPA has been reported to reduce daily sperm production, motility, and count, in addition to damaging the sperm acrosome, weakening the fertilizing ability of sperm, and increasing the likelihood of sexual dysfunction [19,33,81]. In an effort to mitigate the adverse effects of BPA, researchers have explored alternative compounds with similar properties to BPA but with fewer risks to human health and the environment [56,61]. Consequently, some related compounds were adopted for practical use under the assumption that their impact on human health would be less harmful compared to BPA. However, subsequent research revealed that these substitute compounds also have the potential to affect human health adversely [17,61]. Concentrations of bisphenol in industrial zones of Korea, China, Japan, and India have been found to be several times greater than in other areas [42,61,9]. Moreover, the frequent industrial use of BPA analogs poses a serious threat to both human and environmental health. Therefore, this issue has raised serious concerns.

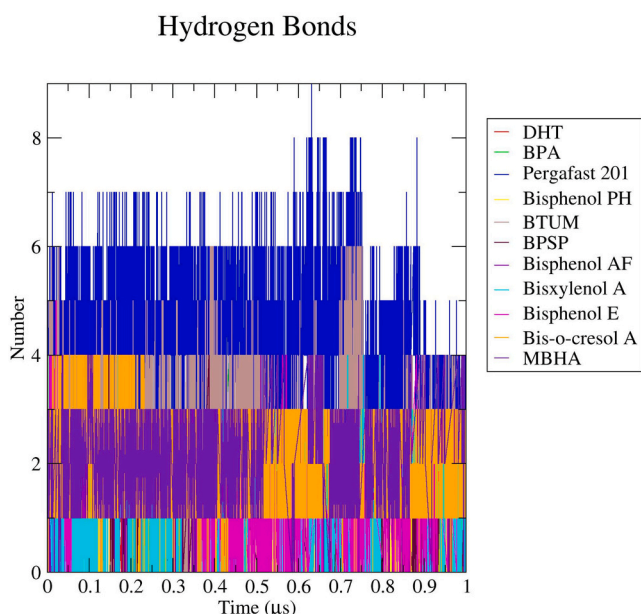


Fig. 6. Number of HBs formed in each complex during the 1 μ s simulations.

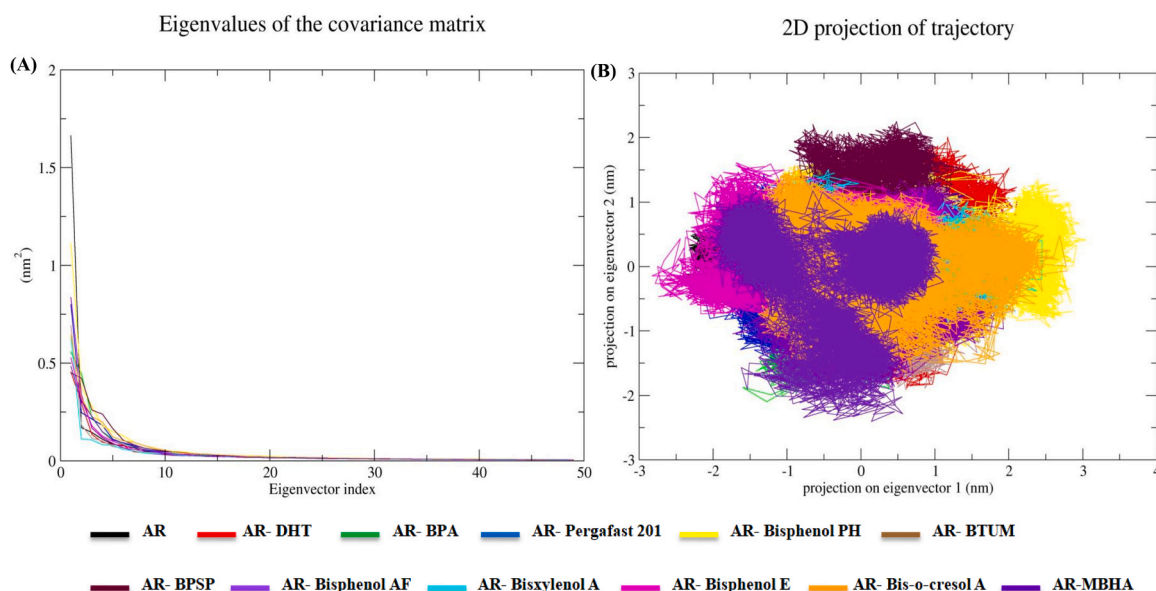


Fig. 7. Essential dynamics analysis. (A) Eigenvalues derived from running each simulation over 1 μ s and used for PCA-depicted eigenvalues vs. the first 50 eigenvectors. (B) The first two eigenvectors represent the AR motion in space for all the systems.

Like BPA, BPA analogs can bind to AR and alter various biological processes associated with this receptor [19,72]. The aim of the present study was to understand how BPA analogs interact with AR. Therefore, molecular docking was conducted to investigate the key interacting amino acid residues of AR and the binding free energy among the BPA analogs with respect to BPA and DHT. Molecular docking analysis is a powerful computational approach that enables the exploration of protein–ligand interactions, the visualization of amino acid residues contributing to interactions through different types of bonding, and the identification of the best pose with minimum binding energy [2]. Furthermore, physicochemical property analysis and toxicity prediction, followed by MDS and FEL, were performed [18,34,74,79].

Through molecular docking, the present study investigated how BPA and its analogs interact with AR, using DHT as a reference. In an earlier investigation, researchers employed a combination of quantitative structure-activity relationship (QSAR), molecular docking, and enzyme assay experiments [82]. The findings indicated that certain analogs of BPA demonstrated stronger inhibitory effects on the activity of human and rat aromatase (CYP19A1), an enzyme with a key role in the catalytic conversion of adrenal androgens. The structures of these analogs may influence their inhibitory strength and their ability to impact estradiol production in intact cells [82]. Studying these interactions has enabled the identification of the 10 most promising BPA analogs, including BPA itself, in relation to AR through molecular docking. It was predicted that out of 10 hazardous compounds, four BPA analogs (Pergafast 201, BPPH, BTUM, and BPSP) exhibit a higher binding affinity with AR in comparison to BPA. However, their binding occurs differently on AR, as revealed during the visualization and analysis of docked complexes. Interestingly, the binding nature of BPA and DHT was observed to be similar.

A previous study reported that BPAF demonstrated toxicity similar to that of BPA through estrogen receptors and aromatase pathways in zebrafish [55]. Therefore, the present study provides valuable insights for further investigating the toxicity of BPA analogs with respect to AR in humans. Moreover, the physicochemical properties of these compounds and their potential toxicity were predicted, which is crucial for evaluating these molecules computationally [50,67]. Most of the selected compounds adhered to Lipinski's rule of five [32], except for BPPH, BTUM, and BXA, which did not fully meet these criteria. Lipinski's rule establishes standards for favorable ADMET properties, including a molecular weight under 500 Da, a $\log P$ value < 5 , a maximum of five HB

donors, and up to 10 HB acceptors [32,74]. Adhering to these guidelines is important because it makes compounds behave similarly to oral medicine, facilitating easy absorption in humans and animals [32]. Furthermore, these analogs possess characteristics that facilitate their passage through cell membranes. The polar surface areas of BPA analogs suggest that they can easily move across cell membranes [36]. Additionally, predictions were made that these BPA analogs might possess harmful properties, including the potential to cause mutations, tumors, and irritation [56].

In the field of computational toxicology and informatics, MDS is recognized as a powerful approach for assessing the behaviors of hazardous chemicals and their interactions with molecular targets in humans and animals, as demonstrated by previous studies [31,46,8]. Here, MDS was used to study the stability of the interaction between BPA and its analogs with AR, comparing it with the docked complex of DHT with AR. This method helps predict how molecular targets will behave before and after binding to any chemical compounds or ligands [23]. When measuring the conformational behavior of AR over time through RMSD analysis, it was found that all complexes exhibited stable trajectories during the simulation (1 μ s), confirming strong interactions between the BPA analogs and AR [18,49]. Furthermore, this was validated by examining structural flexibility, compactness, SASA, and HBs, in addition to conducting PCA and Gibbs FEL analysis. Furthermore, in the experimental validation, only BPA suppressed DHT-induced AR dimerization in the cytosol, similar to the AR-specific antagonist bicalutamide. This disruption by BPA in the cytosol induced the suppression of the translocation of ligand-activated AR to the nucleus, similar to exogenous AR antagonistic substrates, such as azole, organophosphorus pesticides, and carbamate herbicide [20–22]. The present study revealed that the AR-mediated endocrine-disrupting potential of BPA is significantly higher compared to the BPA analogs, which were found to be less effective due to their interaction with different amino acid residues and distinct binding patterns compared to BPA. Computational analysis indicated lower binding energy for these analogs in comparison to BPA. Furthermore, the selected top-four BPA analogs also have higher molecular weights. Based on the obtained results, we can conclude that BPA not only affects the conformation of AR but also disrupts its normal activities. Therefore, this study provides valuable insights into AR-mediated endocrine-disrupting effects by exploring structure-activity relationships and potential therapeutic development [19,54,62,69].

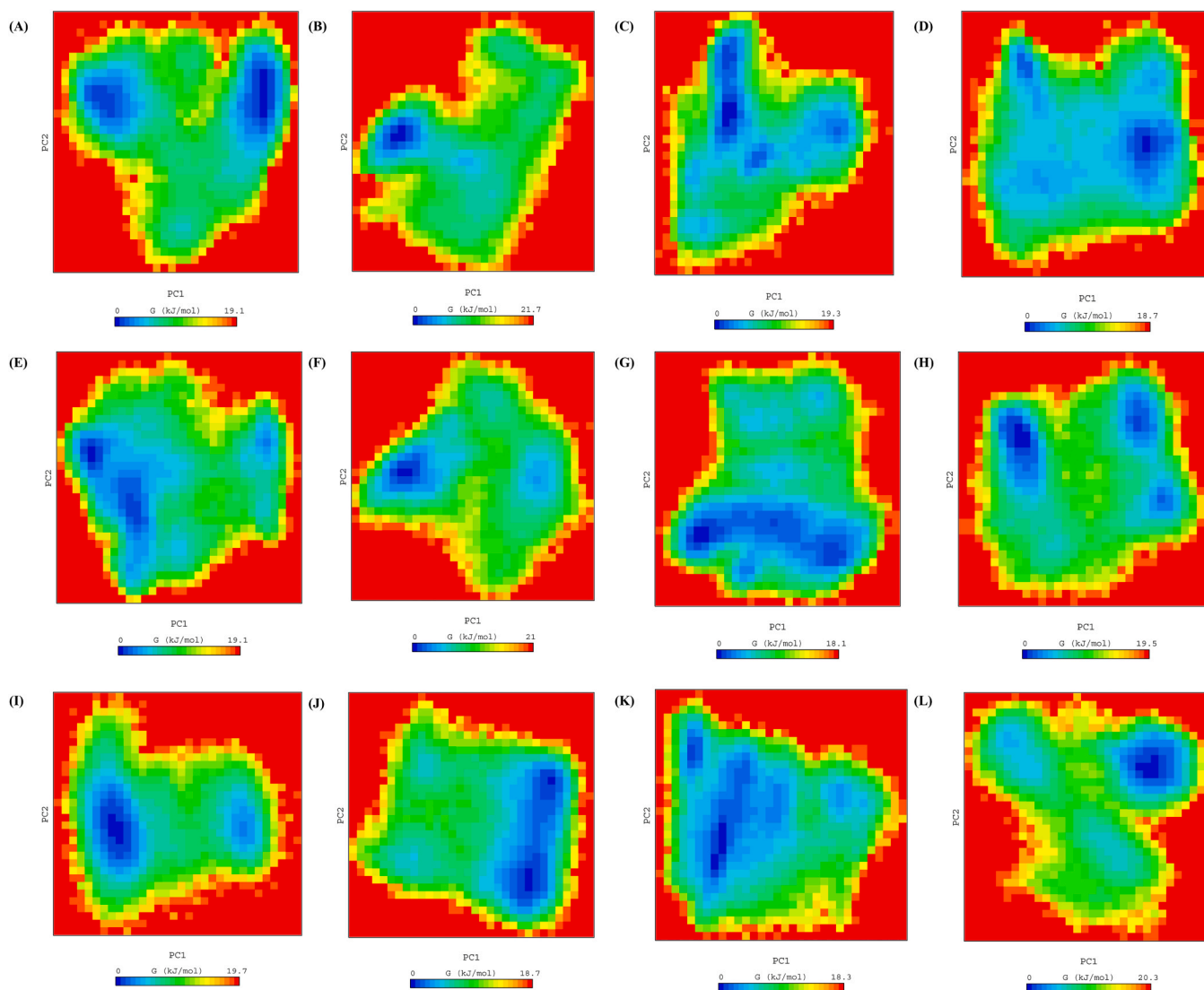


Fig. 8. Color-coded illustration of the Gibbs FEL plotted using PC1 and PC2. The color bar indicates the Gibbs free energies (kJ mol^{-1}) for conformational states with the lowest (blue) and highest (red) energies. (A) AR, (B) AR-DHT, (C) AR-BPA, (D) AR-Pergafast 201, (E) AR-BPPH, (F) AR-BTUM, (G) AR-BPSP, (H) AR-BPAF, (I) AR-BXA, (J) AR-BPE, (K) AR-Bis-*o*-cresol A, and (L) AR-MBHA.

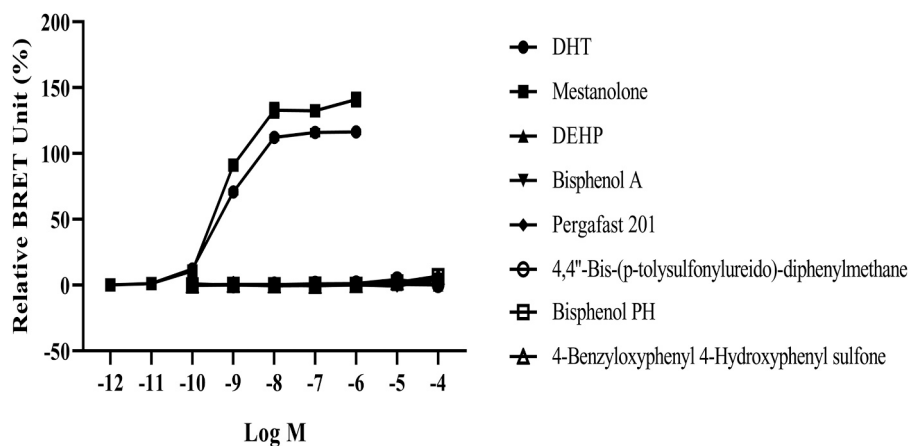


Fig. 9. Concentration–response curves of the AR dimerization affinities of BPA and its four analogs in the BRET-based assay. All the data represent the mean values from three repeats and are presented as mean \pm SD.

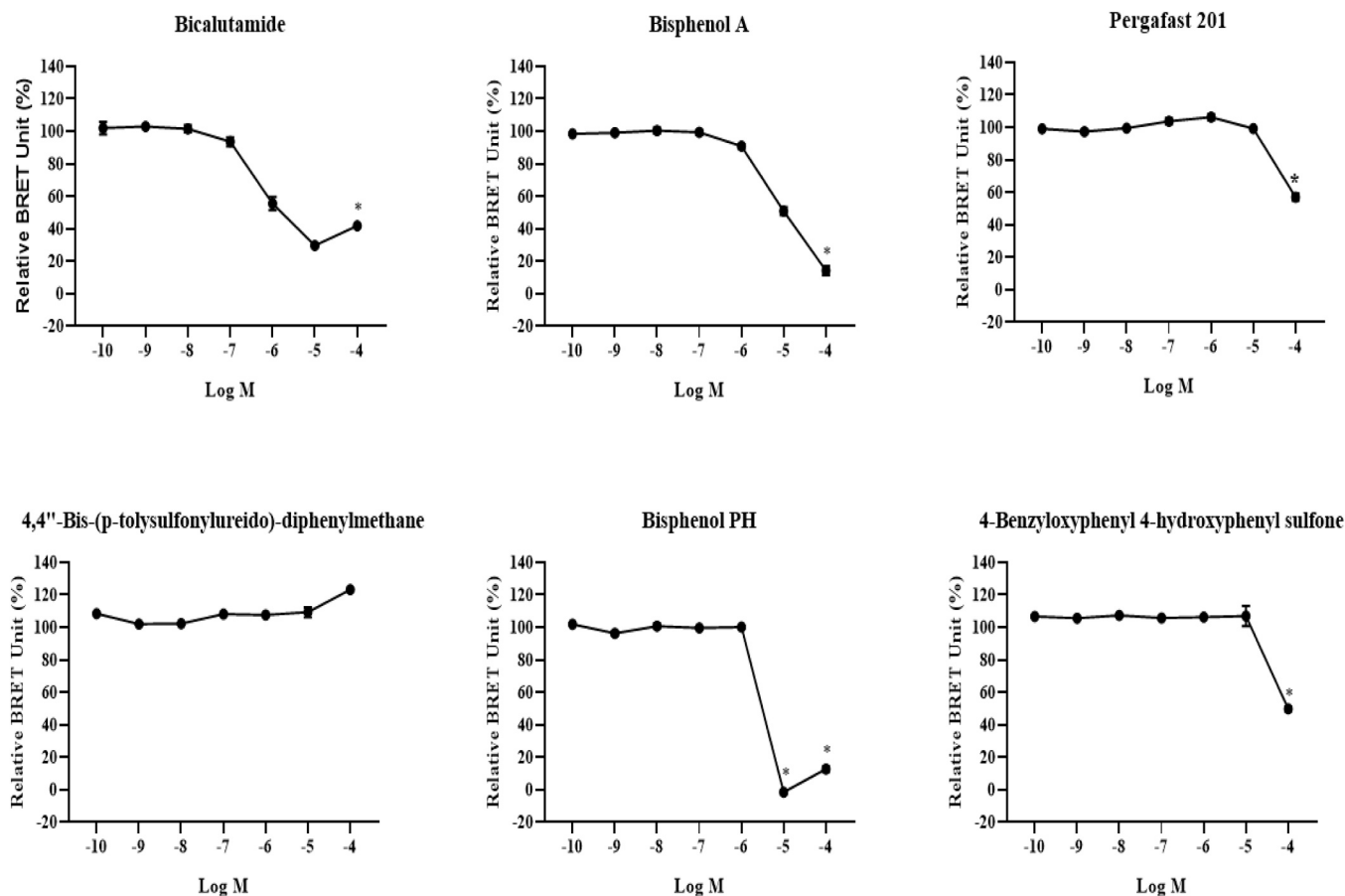


Fig. 10. Concentration–response curves of the AR dimerization affinities of BPA and four BPA analogs in the presence of 800 pMDHT. All the data represent the mean values from three repeats and are presented as mean \pm SD. The asterisks (*) indicate cell viability < 80.0%.

5. Conclusion

In this study, we investigated the interactions between AR and BPA, as well as BPA analogs, in comparison to the natural ligand DHT by using cutting-edge computational methods, including molecular docking, ADMET prediction, MDS, and experimental validation through in vitro BRET-based assays. The binding behavior of BPA to AR is similar to the binding behavior of DHT. However, upon comparing the top-four screened BPA analogs with BPA, it was found that they demonstrated a higher binding affinity to AR despite variations in their binding patterns. Experimental validation results further revealed that BPA demonstrates a higher level of antiandrogenic activity compared to the other selected compounds, indicating distinct binding characteristics compared to both BPA and DHT. This study not only provides insights into the physicochemical and toxicity-related properties of these compounds but also identifies key amino acid residues of AR that contribute to their binding interactions. Consequently, it paves the way for a more in-depth exploration of the toxicity of BPA analogs concerning AR in humans. To the best of our knowledge, this is the first report demonstrating the interaction between different BPA analogs and AR. These results are not only crucial for the scientific community but also bear significance for governance and real-world applications. They can contribute to the development of policies aimed at protecting human health and the environment.

Environmental implication

Human exposure to bisphenol A (BPA) is almost inevitable due to the extensive use of this chemical in various industries and its widespread presence in the environment. Recognized as endocrine disruptors, the

negative impacts of BPA have led to the production of structural analogs. Detected in both environmental and biological samples, their safety remains uncertain, with some behaving like BPA in animal studies. BPA can bind to the androgen receptor (AR) and disrupt its normal activity, directly affecting male fertility. The present study reveals bisphenols-AR molecular interactions, identifying key AR amino acid residues. Findings emphasize bisphenol risks, prompting future interventions.

CRediT authorship contribution statement

Rajesh Kumar Pathak: Conceptualization, Methodology, Software, Formal analysis, Writing - original draft. **Da-Woon Jung:** Methodology, Formal analysis, Validation. **Seung-Hee Shin:** Conceptualization, Validation. **Buom-Yong Ryu:** Conceptualization, Validation. **Hee-Seok Lee:** Conceptualization, Resources, Supervision, Writing - review & editing. **Jun-Mo Kim:** Conceptualization, Resources, Supervision, Writing - review & editing, Project administration, Funding acquisition.

Declaration of Competing Interest

The authors declare that they have no known competing financial interests or personal relationships that could have appeared to influence the work reported in this paper.

Data availability

No data was used for the research described in the article.

Acknowledgments

This research was supported by the Basic Science Research Program through the National Research Foundation of Korea (NRF) funded by the Ministry of Education (NRF-2018R1A6A1A03025159). High-performance computing and other necessary facilities provided by the Chung-Ang University are gratefully acknowledged.

Appendix A. Supporting information

Supplementary data associated with this article can be found in the online version at [doi:10.1016/j.jhazmat.2024.133935](https://doi.org/10.1016/j.jhazmat.2024.133935).

References

- Agarwal, R., Joshi, S.S., 2023. Toxicity of bisphenol in pregnant females: first review of literature in humans. *Cureus* 15 (5), e39168. <https://doi.org/10.7759/cureus.39168>.
- Agnihotry, S., Pathak, R.K., Srivastav, A., Shukla, P.K., Gautam, B., 2020. Molecular docking and structure-based drug design. In: Singh, D.B. (Ed.), *Computer-Aided Drug Design*. Springer, Singapore, pp. 115–131. https://doi.org/10.1007/978-981-15-6815-2_6.
- Aschberger, K., Castello, P., Hoekstra, E., Karakitsios, S., Munn, S., Pakalin, S., Sarigiannis, D., 2010. Bisphenol A and baby bottles: challenges and perspectives. Publications Office of the European Union, Luxembourg.
- Cao, M., Wei, J., Pan, Y., Wang, L., Li, Z., Hu, Y., Liang, Y., Cao, H., 2023. Antagonistic mechanisms of bisphenol analogues on the estrogen receptor α in zebrafish embryos: experimental and computational studies. *Sci Total Environ* 857 (Pt 1), 159259. <https://doi.org/10.1016/j.scitotenv.2022.159259>.
- Carbone, J., Ghidini, A., Romano, A., Gentilucci, L., Musiani, F., 2022. PaDock: a web server for positional distance-based and interaction-based analysis of docking results. *Molecules* 27 (20), 6884. <https://doi.org/10.3390/molecules27206884>.
- Cariati, F., D'Uonno, N., Borrillo, F., Iervolino, S., Galdiero, G., Tomaiuolo, R., 2019. Bisphenol A: an emerging threat to male fertility. *Reprod Biol Endocrinol* 17 (1), 6. <https://doi.org/10.1186/s12958-018-0447-6>.
- Carstensen, L., Zippel, R., Fiskal, R., Börnick, H., Schmalz, V., Schubert, S., Schaffer, M., Jungmann, D., Stolte, S., 2023. Trace analysis of benzophenone-type UV filters in water and their effects on human estrogen and androgen receptors. *J Hazard Mater* 456, 131617. <https://doi.org/10.1016/j.jhazmat.2023.131617>.
- Chen, Y., Tang, H., Cheng, Y., Huang, T., Xing, B., 2023. Interaction between microplastics and humic acid and its effect on their properties as revealed by molecular dynamics simulations. *J Hazard Mater* 455, 131636. <https://doi.org/10.1016/j.jhazmat.2023.131636>.
- Cosentino, S., Aureli, F., Iannilli, V., 2022. Bisphenols A and its analogues induce genotoxic damage in marine and freshwater amphipods. *Environ Adv* 7, 100183. <https://doi.org/10.1016/j.envadv.2022.100183>.
- Cui, X., Zhao, Y., Hao, N., Zhao, W., 2023. A multi-framework for bisphenols based on their high performance and environmental friendliness: Design, screening, and recommendations. *J Hazard Mater* 457, 131709. <https://doi.org/10.1016/j.jhazmat.2023.131709>.
- Davey, R.A., Grossmann, M., 2016. Androgen receptor structure, function and biology: from bench to bedside. *Clin Biochem Rev* 37 (1), 3–15.
- Eberhardt, J., Santos-Martins, D., Tillack, A.F., Forli, S., 2021. AutoDock Vina 1.2.0: new docking methods, expanded force field, and Python bindings. *J Chem Inf Model* 61 (8), 3891–3898. <https://doi.org/10.1021/acs.jcim.1c00203>.
- Estébanez-Perpiñá, E., Moore, J.M., Mar, E., Delgado-Rodríguez, E., Nguyen, P., Baxter, J.D., Buehrer, B.M., Webb, P., Fletterick, R.J., Guy, R.K., 2005. The molecular mechanisms of coactivator utilization in ligand-dependent transactivation by the androgen receptor. *J Biol Chem* 280 (9), 8060–8068. <https://doi.org/10.1074/jbc.M407046200>.
- Forest, V., 2022. Experimental and computational nanotoxicology—Complementary approaches for nanomaterial hazard assessment. *Nanomater (Basel)* 12 (8), 1346. <https://doi.org/10.3390/nano12081346>.
- Forli, S., Huey, R., Pique, M.E., Sanner, M.F., Goodsell, D.S., Olson, A.J., 2016. Computational protein-ligand docking and virtual drug screening with the AutoDock suite. *Nat Protoc* 11 (5), 905–919. <https://doi.org/10.1038/nprot.2016.051>.
- Gao, T., Yin, Z., Wang, M., Fang, Z., Zhong, X., Li, J., Hu, Y., Wu, D., Jiang, K., Xu, X., 2020. The effects of pubertal exposure to bisphenol-A on social behavior in male mice. *Chemosphere* 244, 125494. <https://doi.org/10.1016/j.chemosphere.2019.125494>.
- Harnett, K.G., Chin, A., Schuh, S.M., 2021. BPA and BPA alternatives BPS, BPAF, and TMBPF, induce cytotoxicity and apoptosis in rat and human stem cells. *Ecotoxicol Environ Saf* 216, 112210. <https://doi.org/10.1016/j.ecoenv.2021.112210>.
- Hollingsworth, S.A., Dror, R.O., 2018. Molecular dynamics simulation for all. *Neuron* 99 (6), 1129–1143. <https://doi.org/10.1016/j.neuron.2018.08.011>.
- Huang, X., Cang, X., Liu, J., 2019. Molecular mechanism of Bisphenol A on androgen receptor antagonism. *Toxicol Vitro* 61, 104621. <https://doi.org/10.1016/j.tiv.2019.104621>.
- Jeong, D.H., Jung, D.W., Jang, C.H., Kim, U.J., Park, Y., Park, Y., Lee, H.S., 2023. Chlorpropham, a carbamate ester herbicide, has an endocrine-disrupting potential by inhibiting the homodimerization of human androgen receptor. *Environ Pollut* 325, 121437. <https://doi.org/10.1016/j.envpol.2023.121437>.
- Jung, D.W., Jeong, D.H., Kim, U.-J., Lee, H.-S., 2023. The triazole fungicide metconazole inhibits the homodimerization of human androgen receptors to suppress androgen-induced transcriptional activation. *Chem Biol Interact* 378, 110489. <https://doi.org/10.1016/j.cbi.2023.110489>.
- Jung, D.W., Jeong, D.H., Lee, H.S., 2022. Endocrine disrupting potential of selected azole and organophosphorus pesticide products through suppressing the dimerization of human androgen receptor in genomic pathway. *Ecotoxicol Environ Saf* 247, 114246. <https://doi.org/10.1016/j.ecoenv.2022.114246>.
- Kato, K., Nakayoshi, T., Kurimoto, E., Oda, A., 2021. Molecular dynamics simulations for the protein-ligand complex structures obtained by computational docking studies using implicit or explicit solvents. *Chem Phys Lett* 781, 139022. <https://doi.org/10.1016/j.cplett.2021.139022>.
- Kim, S., Chen, J., Cheng, T., Gindulyte, A., He, J., He, S., Li, Q., Shoemaker, B.A., Thiessen, P.A., Yu, B., Zaslavsky, L., Zhang, J., Bolton, E.E., 2023. PubChem 2023 update. *Nucleic Acids Res* 51 (D1), D1373–D1380. <https://doi.org/10.1093/nar/gkac956>.
- Kojima, H., Takeuchi, S., Sanoh, S., Okuda, K., Kitamura, S., Uramaru, N., Sugihara, K., Yoshinari, K., 2019. Profiling of bisphenol A and eight its analogues on transcriptional activity via human nuclear receptors. *Toxicology* 413, 48–55. <https://doi.org/10.1016/j.tox.2018.12.001>.
- Kumar, M., Chen, H., Sarsaiya, S., Qin, S., Liu, H., Awasthi, M.K., Kumar, S., Singh, L., Zhang, Z., Bolan, N.S., Pandey, A., Varjani, S., Taherzadeh, M.J., 2021. Current research trends on micro- and nano-plastics as an emerging threat to global environment: A review. *J Hazard Mater* 409, 124967. <https://doi.org/10.1016/j.jhazmat.2020.124967>.
- Kumar Reddy, C.P., Manikandavelu, D., Arisekar, U., Ahilan, B., Uma, A., Jayakumar, N., Kim, W., Govarthanan, M., Harini, C., Vidya, R.S., Madhavan, N., Kumar Reddy, D.R., 2023. Toxicological effect of endocrine disrupting insecticide (deltamethrin) on enzymatical, haematological and histopathological changes in the freshwater iridescent shark, *Pangasius hypthalamus*. *Environ Toxicol Pharmacol* 101, 104201. <https://doi.org/10.1016/j.etap.2023.104201>.
- Lee, S., Liao, C., Song, G.-J., Ra, K., Kannan, K., Moon, H.-B., 2015. Emission of bisphenol analogues including bisphenol A and bisphenol F from wastewater treatment plants in Korea. *Chemosphere* 119, 1000–1006. <https://doi.org/10.1016/j.chemosphere.2014.09.011>.
- Lee, S.H., Hong, K.Y., Seo, H., Lee, H.S., Park, Y., 2021. Mechanistic insight into human androgen receptor-mediated endocrine-disrupting potentials by a stable bioluminescence resonance energy transfer-based dimerization assay. *Chem Biol Inter* 349, 109655. <https://doi.org/10.1016/j.cbi.2021.109655>.
- Lin, J., Deng, L., Sun, M., Wang, Y., Lee, S., Choi, K., Liu, X., 2021. An in vitro investigation of endocrine disrupting potentials of ten bisphenol analogues. *Steroids* 169, 108826. <https://doi.org/10.1016/j.steroids.2021.108826>.
- Lin, W., Qin, Y., Ren, Y., 2024. Flunitrazepam and its metabolites induced brain toxicity: Insights from molecular dynamics simulation and transcriptomic analysis. *J Hazard Mater* 465, 133113. <https://doi.org/10.1016/j.jhazmat.2023.133113>.
- Lipinski, C.A., Lombardo, F., Dominy, B.W., Feeney, P.J., 2001. Experimental and computational approaches to estimate solubility and permeability in drug discovery and development settings. *Adv Drug Deliv Rev* 46 (1–3), 3–26. [https://doi.org/10.1016/s0169-409x\(00\)00129-0](https://doi.org/10.1016/s0169-409x(00)00129-0).
- Liu, X., Wang, Z., Liu, F., 2021. Chronic exposure of BPA impairs male germ cell proliferation and induces lower sperm quality in male mice. *Chemosphere* 262, 127880. <https://doi.org/10.1016/j.chemosphere.2020.127880>.
- Machhar, J., Mittal, A., Agrawal, S., Pethe, A.M., Kharkar, P.S., 2019. Computational prediction of toxicity of small organic molecules: state-of-the-art. *Phys Sci Rev* 4 (10), 20190009. <https://doi.org/10.1515/psr-2019-0009>.
- Marchiandi, J., Alghamdi, W., Dagnino, S., Green, M.P., Clarke, B.O., 2024. Exposure to endocrine disrupting chemicals from beverage packaging materials and risk assessment for consumers. *J Hazard Mater* 465, 133314. <https://doi.org/10.1016/j.jhazmat.2023.133314>.
- Matsson, P., Kihlberg, J., 2017. How big is too big for cell permeability. *J Med Chem* 60(5)1662-1664. <https://doi.org/10.1021/acs.jmedchem.7b00237>.
- Meng, X., Su, S., Wei, X., Wang, S., Guo, T., Li, J., Song, H., Wang, M., Wang, Z., 2023. Exposure to bisphenol A alternatives bisphenol AF and fluorene-9-bisphenol induces gonadal injuries in male zebrafish. *Ecotoxicol Environ Saf* 253, 114634. <https://doi.org/10.1016/j.ecoenv.2023.114634>.
- Montes-Grajales, D., Morelos-Cortes, X., Olivero-Verbel, J., 2021. Discovery of new protein targets of BPA analogs and derivatives associated with noncommunicable diseases: a virtual high-throughput screening. *Environ Health Perspect* 129 (3), 037009. <https://doi.org/10.1289/EHP7466>.
- Moon, M.K., 2019. Concern about the safety of bisphenol A substitutes. *Diabetes Metab J* 43 (1), 46–48. <https://doi.org/10.4093/dmj.2019.0027>.
- Morris, G.M., Huey, R., Lindstrom, W., Sanner, M.F., Belew, R.K., Goodsell, D.S., Olson, A.J., 2009. AutoDock4 and AutoDockTools4: automated docking with selective receptor flexibility. *J Comput Chem* 30 (16), 2785–2791. <https://doi.org/10.1002/jcc.21256>.
- Mustieles, V., D'Cruz, S.C., Couderq, S., Rodríguez-Carrillo, A., Fini, J.-B., Hofer, T., Steffensen, I.-L., Dirven, H., Barouki, R., Olea, N., Fernández, M.F., David, A., 2020. Bisphenol A and its analogues: A comprehensive review to identify and prioritize effect biomarkers for human biomonitoring. *Environ Int* 144, 105811. <https://doi.org/10.1016/j.envint.2020.105811>.
- Mustieles, V., Fernández, M.F., 2020. Bisphenol A shapes children's brain and behavior: towards an integrated neurotoxicity assessment including human data. *Environ Health* 19 (1), 66. <https://doi.org/10.1186/s12940-020-00620-y>.

- [43] Computational toxicology. In: Nicolotti, O. (Ed.), 2018. *Methods in Molecular Biology*. Humana Press, New York, NY. <https://doi.org/10.1007/978-1-4939-7899-1>.
- [44] Nowak, K., Jakopin, Z., 2023. *In silico* profiling of endocrine-disrupting potential of bisphenol analogues and their halogenated transformation products. *Food Chem Toxicol* 173, 113623. <https://doi.org/10.1016/j.fct.2023.113623>.
- [45] Páll, S., Zhmurov, A., Bauer, P., Abraham, M., Lundborg, M., Gray, A., Hess, B., Lindahl, E., 2020. Heterogeneous parallelization and acceleration of molecular dynamics simulations in GROMACS. *J Chem Phys* 153 (13), 134110. <https://doi.org/10.1063/5.0018516>.
- [46] Pandit, S., Singh, P., Parthasarathi, R., 2022. Computational risk assessment framework for the hazard analysis of bisphenols and quinone metabolites. *J Hazard Mater* 426, 128031. <https://doi.org/10.1016/j.jhazmat.2021.128031>.
- [47] Pandya, V., Rao, P., Prajapati, J., Rawal, R.M., Goswami, D., 2024. Pinpointing top inhibitors for GSK3 β from pool of indirubin derivatives using rigorous computational workflow and their validation using molecular dynamics (MD) simulations. *Sci Rep* 14 (1), 49. <https://doi.org/10.1038/s41598-023-50992-7>.
- [48] Pathak, R.K., Kim, J.-M., 2024. Structural insight into the mechanisms and interacting features of endocrine disruptor Bisphenol A and its analogs with human estrogen-related receptor gamma. *Environ Pollut* 345, 123549. <https://doi.org/10.1016/j.envpol.2024.123549>.
- [49] Pathak, R.K., Kim, W.-I., Kim, J.-M., 2023. Targeting the PEDV 3CL protease for identification of small molecule inhibitors: an insight from virtual screening, ADMET prediction, molecular dynamics, free energy landscape, and binding energy calculations. *J Biol Eng* 17 (1), 29. <https://doi.org/10.1186/s13036-023-00342-y>.
- [50] Pathak, R.K., Singh, D.B., Sagar, M., Baunthiyal, M., Kumar, A., 2020. Computational approaches in drug discovery and design. In: Singh, D.B. (Ed.), *Computer-Aided Drug Design*. Springer, Singapore, pp. 1–21. <https://doi.org/10.1007/978-981-15-6815-2-1>.
- [51] Pettersen, E.F., Goddard, T.D., Huang, C.C., Couch, G.S., Greenblatt, D.M., Meng, E.C., Ferrin, T.E., 2004. UCSF Chimera—A visualization system for exploratory research and analysis. *J Comput Chem* 25 (13), 1605–1612. <https://doi.org/10.1002/jcc.20084>.
- [52] Proenca, S., Escher, B.I., Fischer, F.C., Fisher, C., Grégoire, S., Hewitt, N.J., Nicol, B., Paini, A., Kramer, N.I., 2021. Effective exposure of chemicals in *in vitro* cell systems: A review of chemical distribution models. *Toxicol Vit* 73, 105133. <https://doi.org/10.1016/j.tiv.2021.105133>.
- [53] Qin, Y., Dey, A., Purayil, H.T., Daaka, Y., 2013. Maintenance of androgen receptor inactivation by S-nitrosylation. *Cancer Res* 73 (22), 6690–6699. <https://doi.org/10.1158/0008-5472.CAN-13-1042>.
- [54] Qiu, L.-L., Wang, X., Zhang, X.-H., Zhang, Z., Gu, J., Liu, L., Wang, Y., Wang, X., Wang, S.-L., 2013. Decreased androgen receptor expression may contribute to spermatogenesis failure in rats exposed to low concentration of bisphenol A. *Toxicol Lett* 219 (2), 116–124. <https://doi.org/10.1016/j.toxlet.2013.03.011>.
- [55] Qiu, W., Liu, S., Chen, H., Luo, S., Xiong, Y., Wang, X., Xu, B., Zheng, C., Wang, K.-J., 2021. The comparative toxicities of BPA, BPB, BPS, BPF, and BPAF on the reproductive neuroendocrine system of zebrafish embryos and its mechanisms. *J Hazard Mater* 406, 124303. <https://doi.org/10.1016/j.jhazmat.2020.124303>.
- [56] Rahman, M.S., Adegoke, E.O., Pang, M.-G., 2021. Drivers of owning more BPA. *J Hazard Mater* 417, 126076. <https://doi.org/10.1016/j.jhazmat.2021.126076>.
- [57] Rampogu, S., Lee, G., Park, J.S., Lee, K.W., Kim, M.O., 2022. Molecular docking and molecular dynamics simulations discover curcumin analogue as a plausible dual inhibitor for SARS-CoV-2. *Int J Mol Sci* 23 (3), 1771. <https://doi.org/10.3390/ijms23031771>.
- [58] Richter, C.A., Birnbaum, L.S., Farabolini, F., Newbold, R.R., Rubin, B.S., Talsness, C.E., Vandenberg, J.G., Walser-Kuntz, D.R., Vom Saal, F.S., 2007. *In vivo* effects of bisphenol A in laboratory rodent studies. *Reprod Toxicol* 24 (2), 199–224. <https://doi.org/10.1016/j.reprotox.2007.06.004>.
- [59] Rifa, R.A., Lavado, R., 2024. Unveiling the next generation of bisphenol analogs and their impact on human health using *in vitro* methods. *Emerg Contam* 10(2), 100296. <https://doi.org/10.1016/j.emcon.2023.100296>.
- [60] Rochester, J.R., Bolden, A.L., 2015. Bisphenol S and F: A systematic review and comparison of the hormonal activity of bisphenol A substitutes. *Environ Health Perspect* 123 (7), 643–650. <https://doi.org/10.1289/ehp.1408989>.
- [61] Rybczynska-Tkaczyk, K., Skóra, B., Szychowski, K.A., 2023. Toxicity of bisphenol A (BPA) and its derivatives in divers [sic] biological models with the assessment of molecular mechanisms of toxicity. *Environ Sci Pollut Res Int* 30 (30), 75126–75140. <https://doi.org/10.1007/s11356-023-27747-y>.
- [62] Salo-Ahen, O.M., Alanko, I., Bhadane, R., Bonvin, A.M., Honorato, R.V., Hossain, S., Juffer, A.H., Kabedev, A., Lahtela-Kakkonen, M., Larsen, A.S., Lescrini, E., Marimuthu, P., Mirza, M.U., Mustafa, G., Nunes-Alves, A., Pansar, T., Saadabadi, A., Singaravelu, K., Vanmeert, M., 2021. Molecular dynamics simulations in drug discovery and pharmaceutical development. *Processes* 9 (1), 71. <https://doi.org/10.3390/pr9010071>.
- [63] Schaduagrath, N., Lampa, S., Simeon, S., Gleeson, M.P., Spjuth, O., Nantasenamat, C., 2020. Towards reproducible computational drug discovery. *J Cheminform* 12 (1), 9. <https://doi.org/10.1186/s13321-020-0408-x>.
- [64] Sendra, M., Štampar, M., Fras, K., Novoa, B., Figueras, A., Žegura, B., 2023. Adverse (geno)toxic effects of bisphenol A and its analogues in hepatic 3D cell model. *Environ Int* 171, 107721. <https://doi.org/10.1016/j.envint.2022.107721>.
- [65] Shamhari, A., Abd Hamid, Z., Budin, S.B., Shamsudin, N.J., Taib, I.S., 2021. Bisphenol A and its analogues deteriorate the hormones physiological function of the male reproductive system: A mini-review. *Biomedicines* 9 (11), 1744. <https://doi.org/10.3390/biomedicines9111744>.
- [66] Sharipov, M., Ju, T.J., Azizov, S., Turayev, A., Lee, Y.-I., 2024. Novel molecularly imprinted nanogel modified microfluidic paper-based SERS substrate for simultaneous detection of bisphenol A and bisphenol S traces in plastics. *J Hazard Mater* 461, 132561. <https://doi.org/10.1016/j.jhazmat.2023.132561>.
- [67] Singh, D.B., Pathak, R.K., 2020. Computational approaches in drug designing and their applications. In: Gupta, N., Gupta, V. (Eds.), *Experimental Protocols in Biotechnology*, Springer Protocols Handbooks. Humana, New York, NY, pp. 95–117. https://doi.org/10.1007/978-1-0716-0607-0_6.
- [68] Siracusa, J.S., Yin, L., Measel, E., Liang, S., Yu, X., 2018. Effects of bisphenol A and its analogs on reproductive health: a mini review. *Reprod Toxicol* 79, 96–123. <https://doi.org/10.1016/j.reprotox.2018.06.005>.
- [69] Sirasanagandla, S.R., Al-Huseini, I., Sakr, H., Moqadass, M., Das, S., Juliana, N., Abu, I.F., 2022. Natural products in mitigation of bisphenol A toxicity: Future therapeutic use. *Molecules* 27 (17), 5384. <https://doi.org/10.3390/molecules27175384>.
- [70] Tachachartvanich, P., Singam, E.R., Durkin, K.A., Furlow, J.D., Smith, M.T., La Merrill, M.A., 2022. *In vitro* characterization of the endocrine disrupting effects of per- and poly-fluoroalkyl substances (PFASs) on the human androgen receptor. *J Hazard Mater* 429, 128243. <https://doi.org/10.1016/j.jhazmat.2022.128243>.
- [71] Tarafdar, A., Sirohi, R., Balakumaran, P.A., Reshmy, R., Madhavan, A., Sindhu, R., Binod, P., Kumar, Y., Kumar, D., Sim, S.J., 2022. The hazardous threat of Bisphenol A: toxicity, detection and remediation. *J Hazard Mater* 423 (Pt A), 127097. <https://doi.org/10.1016/j.jhazmat.2021.127097>.
- [72] Teng, C., Goodwin, B., Shockley, K., Xia, M., Huang, R., Norris, J., Merrick, B.A., Jetten, A.M., Austin, C.P., Tice, R.R., 2013. Bisphenol A affects androgen receptor function via multiple mechanisms. *Chem Biol Interact* 203 (3), 556–564. <https://doi.org/10.1016/j.cbi.2013.03.013>.
- [73] Trott, O., Olson, A.J., 2010. AutoDock Vina: improving the speed and accuracy of docking with a new scoring function, efficient optimization, and multithreading. *J Comput Chem* 31 (2), 455–461. <https://doi.org/10.1002/jcc.21334>.
- [74] Turner, J.V., Agatonovic-Kustrin, S., 2007. *In silico* prediction of oral bioavailability. In: Testa, B., van de Waterbeemd, H. (Eds.), *Comprehensive Medicinal Chemistry II ADME Tox Approaches*, v.5. Elsevier Ltd, United Kingdom, pp. 699–724. <https://doi.org/10.1016/b0-08-045044-x/00147-4>.
- [75] Van Der Spoel, D., Lindahl, E., Hess, B., Groenhof, G., Mark, A.E., Berendsen, H.J., 2005. GROMACS: fast, flexible, and free. *J Comput Chem* 26 (16), 1701–1718. <https://doi.org/10.1002/jcc.20291>.
- [76] Vandenberg, L.N., Chahoud, I., Heindel, J.J., Padmanabhan, V., Paumgartner, F.J., Schoenfelder, G., 2010. Urinary, circulating, and tissue biomonitoring studies indicate widespread exposure to bisphenol A. *Environ Health Perspect* 118 (8), 1055–1070. <https://doi.org/10.1289/ehp.0901716>.
- [77] Wan, Y.-P., Ma, Q.-G., Hayat, W., Liu, Z.-H., Dang, Z., 2023. Ten bisphenol analogues in Chinese fresh dairy milk: high contribution ratios of conjugated form, importance of enzyme hydrolysis and risk evaluation. *Environ Sci Pollut Res Int* 30 (37), 88049–88059. <https://doi.org/10.1007/s11356-023-28737-w>.
- [78] Wang, Y., Zhong, Z., Chen, X., Sokolova, I., Ma, L., Yang, Q., Qiu, K., Khan, F.U., Tu, Z., Guo, B., Huang, W., 2024. Microplastic pollution and ecological risk assessment of Yueqing Bay affected by intensive human activities. *J Hazard Mater* 461, 132603. <https://doi.org/10.1016/j.jhazmat.2023.132603>.
- [79] Wu, F., Zhou, Y., Li, L., Shen, X., Chen, G., Wang, X., Liang, X., Tan, M., Huang, Z., 2020. Computational approaches in preclinical studies on drug discovery and development. *Front Chem* 8, 726. <https://doi.org/10.3389/fchem.2020.00726>.
- [80] Xue, H., Li, J., Xie, H., Wang, Y., 2018. Review of drug repositioning approaches and resources. *Int J Biol Sci* 14 (10), 1232–1244. <https://doi.org/10.7150/ijbs.24612>.
- [81] Yadav, S.K., Bijalwan, V., Yadav, S., Sarkar, K., Das, S., Singh, D.P., 2023. Susceptibility of male reproductive system to bisphenol A, an endocrine disruptor: Updates from epidemiological and experimental evidence. *J Biochem Mol Toxicol* 37 (4), e23292. <https://doi.org/10.1002/jbt.23292>.
- [82] Zheng, J., Chen, S., Lu, H., Xia, M., Wang, S., Li, X., Li, H., Wang, Y., Ge, R.-s., Liu, Y., 2024. Enhanced inhibition of human and rat aromatase activity by benzene ring substitutions in bisphenol A: QSAR structure-activity relationship and *in silico* docking analysis. *J Hazard Mater* 465, 133252. <https://doi.org/10.1016/j.jhazmat.2023.133252>.
- [83] Zhou, Z.X., Lane, M.V., Kempainen, J.A., French, F.S., Wilson, E.M., 1995. Specificity of ligand-dependent androgen receptor stabilization: receptor domain interactions influence ligand dissociation and receptor stability. *Mol Endocrinol* 9 (2), 208–218. <https://doi.org/10.1210/mend.9.2.7776971>.
- [84] Zoete, V., Cuendet, M.A., Grosdidier, A., Michielin, O., 2011. SwissParam: a fast force field generation tool for small organic molecules. *J Comput Chem* 32 (11), 2359–2368. <https://doi.org/10.1002/jcc.21816>.